

A search for Be stars in multiple systems within the solar neighborhood

V. M. KALARI,¹ R. SALINAS,² C. SÁEZ-CARVAJAL,^{3,1} R. D. OUDMAIJER,^{4,5} S. HOWELL,⁶ S. CABALLERO-NIEVES,⁷ K. KAMP,⁷ R. MATSON,⁸ N. SCOTT,⁹ T. CAO,¹⁰ Z. HARTMAN,⁶ AND H. KIM¹

¹*Gemini Observatory/NSF's NOIRLab, Casilla 603, La Serena, Chile*

²*Nicolaus Copernicus Astronomical Center, Polish Academy of Sciences, Bartycka 18, 00-716 Warszawa, Poland*

³*Instituto de Física y Astronomía, Universidad de Valparaíso, Av. Gran Bretaña 1111, 5030 Casilla, Valparaíso, Chile*

⁴*Royal Observatory of Belgium, Ringlaan 3, B-1180 Brussels, Belgium*

⁵*School of Physics & Astronomy, University of Leeds, Woodhouse Lane, Leeds LS2 9JT, UK*

⁶*NASA Ames Research Center, Moffett Field, CA 94035, USA*

⁷*Embry-Riddle Aeronautical University, Daytona Beach FL*

⁸*U.S. Naval Observatory, 3450 Massachusetts Avenue NW, Washington, D.C. 20392, USA*

⁹*The CHARA Array of Georgia State University, Mount Wilson Observatory, Mount Wilson, CA 91023, USA*

¹⁰*Department of Astronomy, Xiamen University, 422 Siming South Road, Xiamen 361005, Peoples Republic of China*

ABSTRACT

Be stars are widely considered to be the product of binary interaction. However, whether all Be stars are formed via binary interaction is unclear, and detailed estimates of the multiplicity of Be stars and characterization of their components are required. In this study, we present speckle observations of 76 Be stars taken using the Gemini North and South speckle imagers spanning angular separations of 20 mas–1.2'', reaching contrasts $\Delta m \sim$ 5–6 mag at separations around 0.1''. We identify 11 (6 previously unreported) binaries having separations in the 10–1000 au range, and Δm between 0.8–5 mag in our sample. Using archival data to search for components outside our visibility range, we add further multiples (16), which include three triples, leading to a total of 24 multiple systems. Our findings rule out a multiplicity fraction $>27\%$ at the 3σ level within the speckle observations separation range and detection limits. Future homogeneous spectroscopic/interferometric observations are essential to probe the inner separations, and along with analysis of available astrometry can cover the entire separation range to characterize the multiplicity fraction, and evolutionary scenario of Be stars.

Keywords: Be stars – Binary stars – Speckle interferometry – Multiple star evolution

1. INTRODUCTION

Classical Be stars (CBe) are non-supergiant B spectral-type stars with Balmer emission lines (Rivinius et al. 2013). The emission lines arise from a gaseous circumstellar decretion disk, thought to have formed via rapid rotation (e.g. Rivinius & Klement 2024). Be stars are involved in many exotic astrophysical systems, such as X-ray binary stars (Be stars with a neutron star companion), stripped stars (Be stars with a massive, hot companion that has lost its outer envelope and is He-rich), γ Cas stars (highly variable stars with strong X-ray emission). Characterizing Be stars therefore helps better understand a variety of astrophysical phenomena, however, the formation and evolution of Be stars still poses some open questions.

In the past decades, there have been multiple studies constraining the binary statistics of Be stars using

either high-resolution imaging (Abt & Cardona 1984; Mason et al. 1997; Oudmaijer & Parr 2010; Horch et al. 2020; Hutter et al. 2021; Klement et al. 2024; Dodd et al. 2024; Souza et al. 2020; Guerrero et al. 2025), SED analysis (Klement et al. 2021b), or compilations of high-resolution spectroscopic data (Bodensteiner et al. 2020a; Abt & Levy 1978), and searches for post-interaction binary products such as runaways (Boubert & Evans 2018; Berger & Gies 2001). These studies canvass an important space in the separation/period region of Be stars. But, are limited to probing only close binaries using spectroscopy, or more distant ones using classical seeing-limited imaging techniques (see Fig. 1 for illustrative limits). Speckle imaging allows to search for companions located at angular separations not possible via these methods.

In this paper, we attempt to constrain the multiplicity fraction, and properties of companions of known CBe

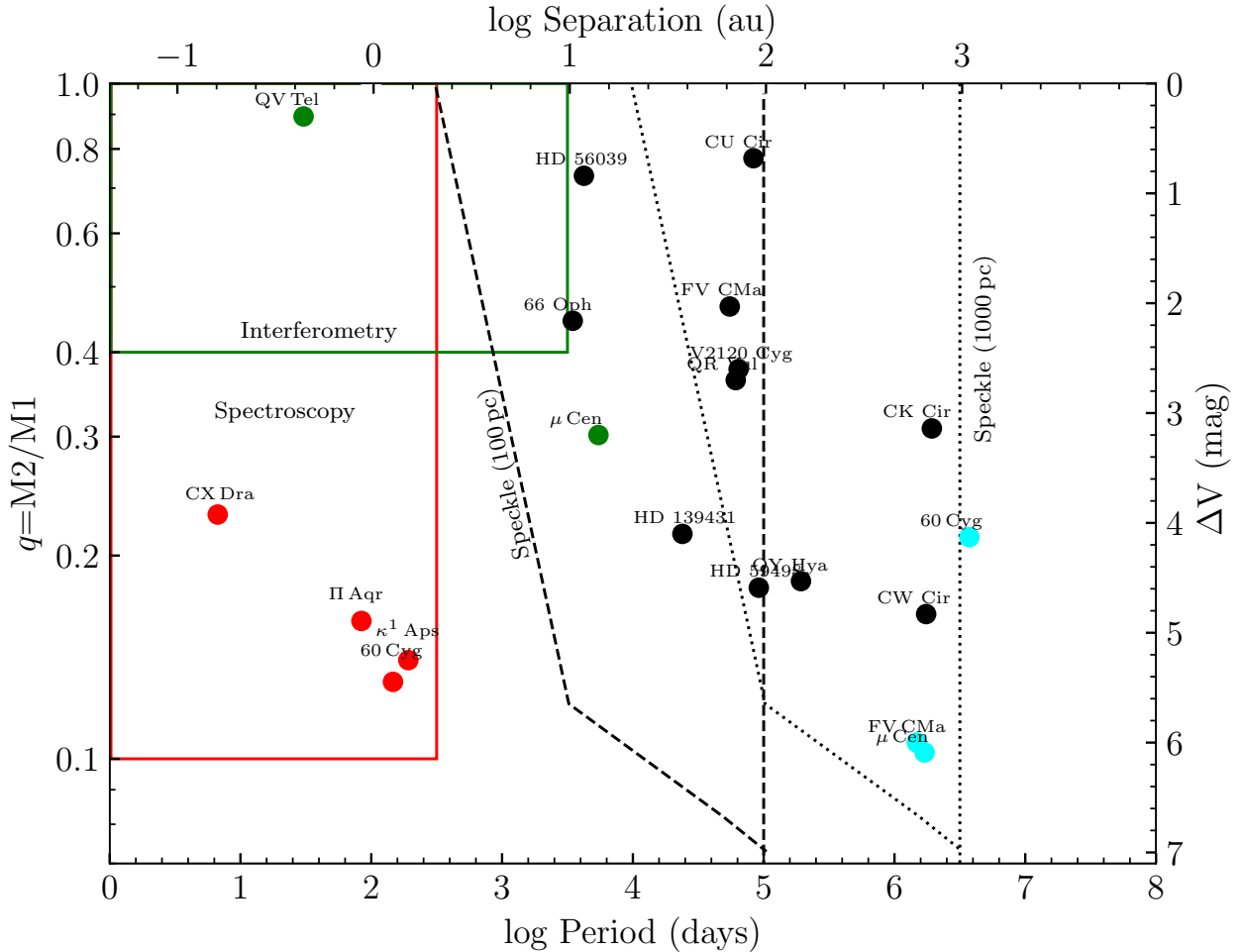


Figure 1. The parameter space of detection limits for various methods, adapted from Hutter et al. (2021). The approximate conversion between the mass ratio, and ΔV were computed assuming a B0V primary from Pecaut & Mamajek (2013). The separation and period relation is computed for a B2V/B5V binary, with no eccentricity. For spectroscopy detection limits, we adopt Sana et al. (2009) where the binary detection probability drops beyond a year for their simulations of massive stars. The dashed and dotted lines represent the speckle detection limits (20 mas–1.2'') at distances of 100, and 1000 pc (approx. distances of stars in this study). The complementarity of different methods in discovering binaries is showcased here. Also shown are detected binaries in our sample from speckle imaging presented in this work (black circles), literature spectroscopy (red circles), archival seeing-limited imaging observations (cyan circles) and interferometric (green) observations. Note that the limits shown here are illustrative, and depend on the exact instrumental configuration for each case.

stars within the local volume of 1 kpc homogeneously, at binary separations between few to 1000 au (Fig. 2), depending on the distance of the source. This corresponds approximately to periods between a few years to a few thousand years for equal mass, early B-type binaries with circular orbits. Our data comes from speckle imaging obtained with either the ‘Alopeke instrument on the Gemini North, or Zorro on the Gemini South twin 8.1 telescopes which allow for a uniform, homogeneous sample with characterized biases allowing for a statistical inference of our results. Our work complements multiplicity fraction estimates from both spectroscopy (which typically probes much smaller separations), clas-

sical seeing-limited imaging or astrometry (at larger separations), and interferometry (which is usually limited to very bright magnitudes, $V \lesssim 8$).

Our paper is organized thus— in section 2 we present the data used in this study while discussing the sample selection, and biases. Section 3 contains our results on the detected multiplicity fraction, literature cross-matches, and nature of companions. Finally, in Section 4 a discussion on the implications of our results within the current literature and favored Be formation scenario is presented.

2. DATA

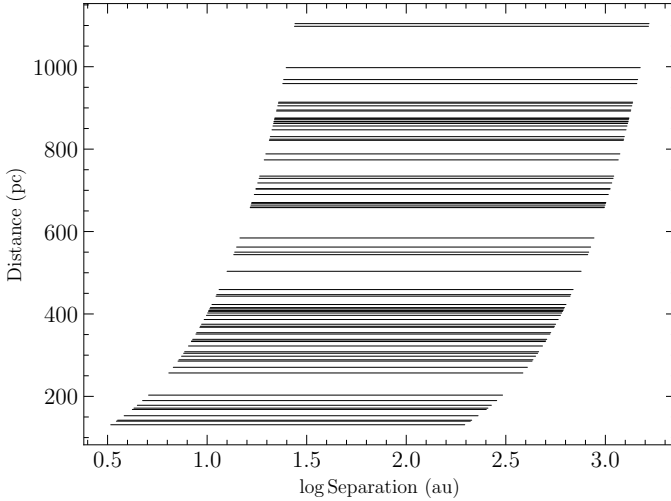


Figure 2. The upper and lower limits of separation range from the primary captured by the speckle observations, as a function of distance. Distances are taken from *Gaia* EDR3 data of Bailer-Jones et al. (2021).

2.1. Observations and data reduction

Our input sample is based on known CBe stars located within 1 kpc. We selected all CBe stars found in the BeSS database¹, which contains 2381 such objects (out of a total 2455 Be stars; 8 stars were marked as Classical/Herbig and not considered). Of these, we selected only those stars having known spectral types between B0-B5 (1265), and cross-matched them with *Gaia* DR2 (Gaia Collaboration et al. 2018) using a radius of 0.3'' (1101), which was the latest catalog available at the time of observation preparation. Stars having parallaxes (accounting for the zero-point offset of 29 μ as; Lindegren et al. 2018) larger than 1 mas (i.e. located at a distance smaller than 1000 pc) were selected (341). Three stars located in the Magellanic Clouds were removed (we assumed that *Gaia* DR2 parallaxes are erroneous here). Since CBe stars within the local volume of 1 kpc are selected, no magnitude criteria were applied. The final database consisted of 338 CBe stars which formed our observational sample. All selection catalogs are available from the author on request.

Data for our targets were collected between March 2020 and September 2021, using the twin speckle imagers Zorro and ‘Alopeke, mounted on the Gemini South, and Gemini North 8.1m telescopes, respectively (Scott et al. 2021), and cover the whole sky (see Fig. 3). The observations are taken in custom medium-band speckle filters in a blue and red channel simultaneously (separated at 674 nm by a dichroic). They are cen-

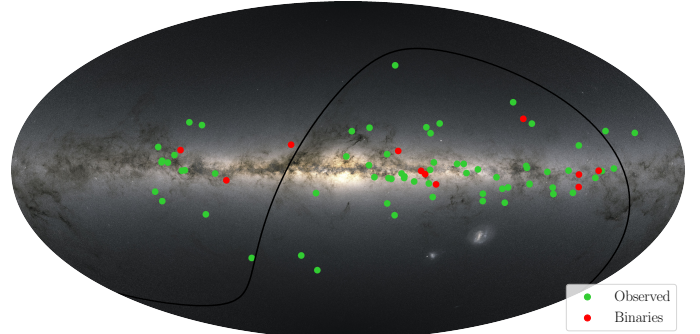


Figure 3. Projection of observed targets on all-sky DSS image. Speckle identified binaries are marked.

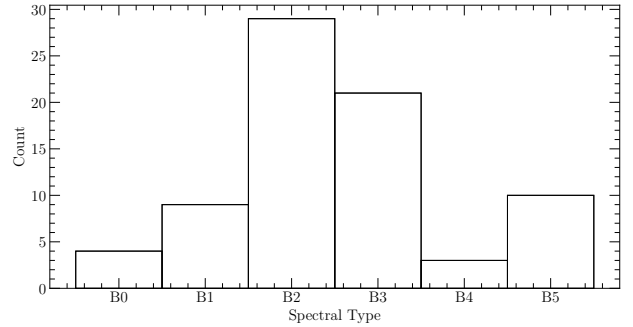


Figure 4. Histogram of spectral types for all observed targets.

tered at either 466 (EO466) and 716 nm (EO716), or at 562 (EO562) and 832 nm (EO832). Observations were taken under zenith seeing of less than 0.7'' in clear skies, though with varying moon phases throughout the period. The observations were spread across a two-year period, but not all of the initially selected targets could be observed due to difficulties in scheduling, weather constraints, and the pandemic. The final list of observed targets, along with their known magnitudes and other relevant identifications, is provided in Appendix A. These data represent a subset of the initially selected targets, reflecting the observational challenges and scheduling limitations encountered during the campaign. In total, 76 CBe targets are studied here, representing \sim 21% of the known CBe stars within a 1 kpc volume. Their spectral types are given in Fig. 4.

Observations taken at Zorro between March–September 2021, were only taken in the 832 nm filter due to an issue with blue camera. For these targets, only red speckle imaging is available, which cannot be used for color comparisons of any companion, or estimating stellar properties. All data were processed using the Howell et al. (2011) pipeline. The pipeline was first developed by Horch et al. (2001) in which the main Fourier analysis is discussed. Using methods and discussions highlighted

¹ <http://basebe.obspm.fr/>

in Tokovinin et al. (2010), Horch et al. (2011) and Howell et al. (2011) provide further details of the methods and the data products which result from the pipeline.

There has not been detected any loss of resolution in the blue channel with the usual narrow band filters we use, as all observations occur at high elevations on purpose. There may be a small loss in a SDSS/broad band filter in the blue, but we rarely use such filters.

We describe briefly the process here. During the reduction, the power spectrum of each image is calculated, and then is corrected for the speckle transfer function by dividing the mean power spectrum of the target by that of the standard star. The pipeline also produces reconstructed images of each target. Fourier analysis is used to identify any multiples in the co-added power spectrum, from any detected fringes. If identified, a fit is used to estimate the angular separation, position angle and magnitude difference. The achieved angular resolutions reached the diffraction limit of the 8.1m telescope. The angular resolutions for the filters EO466, EO532, EO716, and E832 are 15, 17, 22, and 25 mas, respectively. The contrast (Δm) limits for each target were determined.

The method used to compute the contrast curves is described in detail in Horch et al. (2011). Here we give a brief overview. The curves are computed in the filters observed by examining the minimum and maximum background values in annuli centered on the primary star. The contrast curves then dictate the observational limit for detecting close companions in relative magnitude compared to the primary star magnitude, as a function of angular separation. A representative reconstructed image, and the corresponding contrast curve of 66 Oph is shown as an example in Fig. 5. The spline fit to the 5σ contrast curve starts with a forced linear segment from the diffraction limit and $\Delta m=0$, to the 5σ background fit at $0.1''$. This is not a realistic inner contrast limit, but is adopted for spline fitting. To see a realistic set of detections, for example showing that the inner contrast curves do reach the refraction limit, see Fig. 3 in Lester et al. (2021), where there are companion detections “inside” the spline fit along the diffraction limit. Additionally, using multiple close-in companion detections, the true contrast curve between this region was shown to reach the diffraction limit by Howell et al. (2025). Finally, there has not been detected any loss of resolution in the blue channel with the usual narrow band filters used for these observations, and all observations occur at high elevations on purpose as detailed in Appendix A. While there may be a small loss in a broad-band filter in the blue, we do not use such filters for our observations.

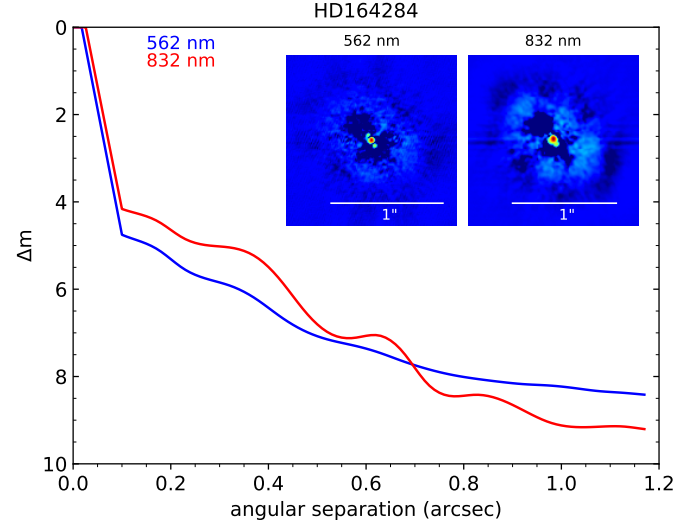


Figure 5. Reconstructed image of 66 Oph in the speckle EO832 filter. The contrast curves for that filter, and the bluer EO562 filter are shown. The companion is visible close to the binary, around 50 mas away, at a position angle of 211° (a 180° ambiguity exists in the position angle of the companion).

All datasets in the raw format are available publicly from the Gemini archive², and in the reduced format on the NASA-ExoFOP webpage³, which includes all reconstructed images, contrast curves, and multiple properties (if present).

2.2. Effect of runaway stars in the sample

Finally, we also checked for potential runaways in our sample. We used Gaia Collaboration et al. (2023) astrometry to compute the peculiar tangential velocities (v_t)_{pec} of our sample stars using the recipe and reference values of Kalari et al. (2019). We find no stars meeting previously used threshold of runaways adopted for early type stars by Moffat et al. (1998) of 42 km s^{-1} . Using a more relaxed criteria of $>30 \text{ km s}^{-1}$ from Cruz-González et al. (1974) for peculiar radial velocities (v_r)_{pec}, we find one star, GP Vir. GP Vir exhibit's $(v_t)_{\text{pec}} = 30 \text{ km s}^{-1}$; and has a measured $(v_r)_{\text{pec}}$ from Gaia Collaboration et al. (2023) radial velocity of 39 km s^{-1} . We report it as the only runaway candidate in our sample, and suggest the effect of runaways on reported multiplicity statistics of our sample computed using available data is negligible.

2.3. Sample incompleteness

² <https://archive.gemini.edu>

³ <https://exofop.ipac.caltech.edu/>

Our sample, while volume-limited, is not magnitude limited since most Be stars are within the instrumental detection limit (all stars selected to be observed have $V < 12$ mag). As a test of our sample incompleteness, we compute the ratio of the volume of a given object with respect to the maximum volume, v/v_{\max} (Schmidt 1968) using the *Gaia* DR2 parallaxes adopted for target selection. Given the thickness of the Galactic disc, the numbers are expected to increase as the square of the distance (d^2) beyond ~ 100 pc, and this is also shown for the sample. For a uniform distribution, the mean of this value should be close to 0.5, however for our sample this is around 0.25. This can be visualized in the distribution of volume of our sources (Fig. 6), which are clustered closer towards us for both the observed and target samples.

We interpret this as a lack of distant Be stars in our sample, but also as a lack of known Be stars outside the solar neighborhood. This may suggest that the vast majority of Be stars beyond the solar neighborhood ($\gtrsim 100$ pc) remain uncatalogued, and that future studies to detect them homogeneously (for e.g. using their emission lines using methods described in Vioque et al. 2020; Kalari 2019, or infrared excesses as shown by Chen et al. 2016) may be necessary to see if these are to be found. Such studies are essential precursors for future statistical analyses regarding CBe stars.

2.4. Effect of parallax cuts

We note that using *Gaia* DR2 parallaxes might bias against resolved binaries, since they may not always have *Gaia* DR2 astrometry (Gaia Collaboration et al. 2018). To estimate the impact of this on our final sample, we inspected the catalog of 164 B0-B5 spectral types not having *Gaia* DR2 parallaxes. We applied a magnitude cut of $V < 12$ mag (which is the faintest magnitude in our selected sample) giving us 71 stars. Out of these, the majority (~ 60) are located along the Galactic plane in known open associations, particularly χ Persei, and Carina that are beyond 1 kpc. They appear most likely Be star members of clusters that are beyond 1 kpc. We then inspected archival parallaxes from the SIMBAD database⁴, and found only 6 stars with parallaxes > 1 mas (which were also not close to aforementioned clusters), of which four are very bright $V < 3$ mag (γ Cas, δ Sco, ζ Tau, η Cen) hence not having *Gaia* data, and the remaining two are HD 75925, HD 72067. Out of these, HD 72067 and δ Sco have close binaries from the Washington Double star catalog (Mason et al. 2022).

⁴ <https://simbad.u-strasbg.fr/simbad/sim-fbasic>

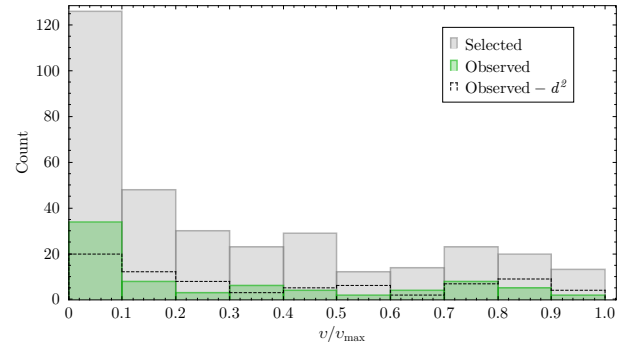


Figure 6. v/v_{\max} of all the selected CBe stars with spectral types between B0-B5 having *Gaia* DR2 parallaxes > 1 mas found in the BeSS database, and also the observed sample. The dotted histogram represents the d^2/d_{\max}^2 values for the observed sample.

Overall, we note that two known close binaries, and six potential binaries may have been missed because of our *Gaia* DR2 parallax criteria, and the effect is not statistically significant.

3. ANALYSIS

3.1. Speckle binaries

We have obtained speckle imaging reaching around 20 mas with contrasts (Δm) between 1-5 mag of 76 Be stars tabulated in Appendix A. Our results are described below, with a discussion on specific objects given in Appendix B.

Of our 76 targets, 11 displayed evidence for a companion using speckle imaging. No higher order multiples were detected. The properties of the binary companions are given in Table 1. To estimate the chance of spurious contaminants, we follow Correia et al. (2006); Pomohaci et al. (2019), where the chance of spurious contaminants (P_C) is given by $1 - e^{-\pi d^2 \rho}$, where d is the angular separation, and ρ the background source density. ρ is computed using *Gaia* DR3 photometry assuming a circle of 1 arcmin² centered on the primary, with the magnitude limit set to $G < 18$ mag. None of the sources had $P_C > 5\%$, with all less than 1%, except CW Cir (HD 134958) and CK Cir (HD 128293) at 1.2 and 3.8% respectively. We thus conclude that none of the detected binaries are chance superpositions in our sample. In Table 1, we give the angular separation in arcsec, and based on the *Gaia* DR3 distance (Bailer-Jones et al. 2021) the separation in au. The reported position angle is given, although some stars may have a 180° ambiguity (see Howell et al. 2011). The Δm is given in the EO 832 filter unless specified, with a detailed explanation of each binary found in Appendix B. All of the binaries are within 1000 au. These are all detached

binaries based on their separation (with periods greater than a few thousand days), i.e. not directly interacting.

3.1.1. Monte Carlo simulations

Following Kalari et al. (2024), we estimate using Monte Carlo simulations the masses of potentially undetected companions, using the tool described in Wood et al. (2021). For each source, we extracted the contrast curve in the filter data was taken (only for the red camera) in, and adopted a mass following the spectral type-mass relationship given in Pecaut & Mamajek (2013). The period and mass ratio distribution of early-type stars is not as well characterized as low-mass stars due to observational limitations (Wood et al. 2021). We adopt a log-normal period distribution, with a peak at 1000 days, and slope for the mass ratio distribution, γ of -1.7 for mass ratios, $q > 0.3$, and σ of 2.28 following the constraints found for early-type B stars by Moe & Di Stefano (2017). Uniform orbital inclination, and eccentricity was assumed. For each source, 5 million companions were generated, and the magnitude was computed using the Dotter (2016) stellar models.

In Fig. 7 the resulting average detection probability in each filter, along with the spread is shown. The 3σ detection probability limits are shown for a given companion mass as a function of the orbital period and separation. As this is estimated using the speckle contrast curve, under the estimated detection limit is the parameter space where a companion is unlikely to be detected using our speckle imaging. This shows via alternative means the discovery parameter space of speckle imaging observed in Fig. 1. Companions between 10 to a few 100 au can be recovered by speckle imaging for this sample to around mass ratios of 0.8, while closer-in or further out companions are missed. Low mass ratio close-in binaries have a low probability of detection using speckle, and we cannot statistically rule out binaries in that space using our current observations, but can rule out with high confidence any binaries within ~ 50 –200 au having $q > 0.8$ for the vast majority of our sample, that have been undetected. The complete set of accompanying recovery fractions for each object can be obtained from the principal author on request.

3.2. Comparison with literature

The limitation of our observations are both in separation ranges (20 mas to $\sim 1.2''$), and in contrast ratios, as depicted in Fig. 1. The resulting multiple fraction, and detected multiple fall within these limits. However, other observational methods allow for detecting close-in (spectroscopy/interferometry), or further (classical seeing-limited imaging, astrometry) sources. Here, we consolidate our detected binaries with available archival

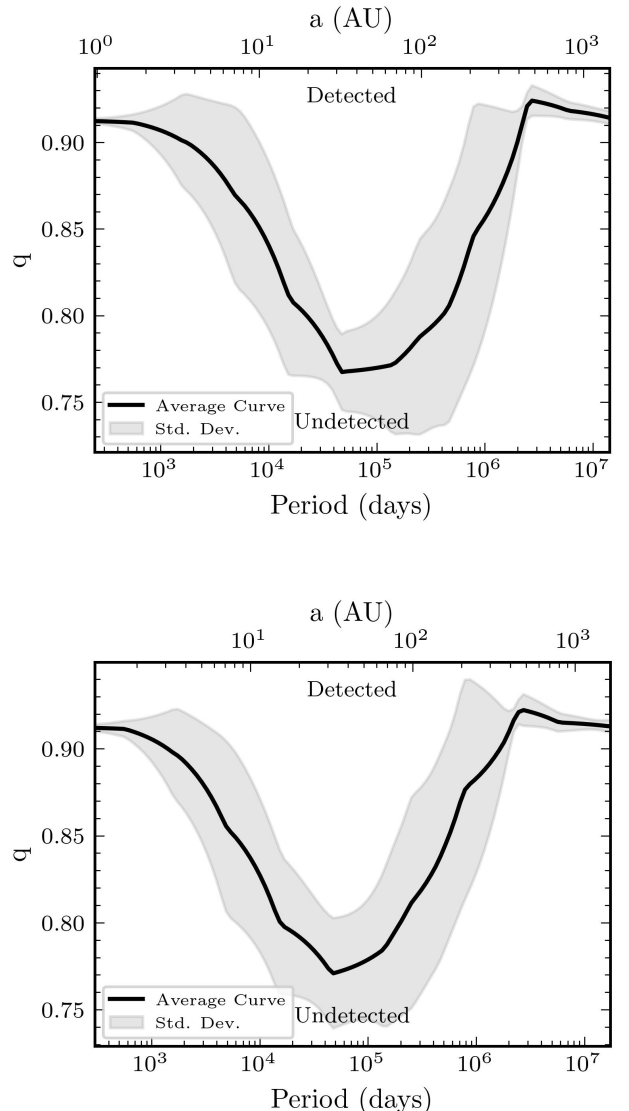


Figure 7. Averaged detection limits for companions around Be stars computed using the contrast curves, and converted to mass ratios assuming Dotter (2016) stellar models for the EO 716 (top) and EO 832 filters (bottom). Gray shaded regions describe the variation among the detection limits.

information based on classical, or interferometric imaging and spectroscopy.

3.2.1. WDS catalog counterparts

To assess if we are missing companions beyond our separation range, we compare our results to the WDS (Washington Double star) Catalog from Mason et al. (2022). Cross-matching with the identifiers to the J2000 epoch, we find 30 unique companions, which are re-

Table 1. Properties of multiples detected in our study

Name	Sp. type	Δm^1	Sep. (mag)	Sep. (au)	P.A. ($''$)	Dist. ² (pc)	Epoch (MJD)
FV CMa	B2Vnne	2.03	65.4	0.089	198.6	734.5	59227.251748
HD 56039	B5Ve	0.84 ⁴	11.8	0.021	193.2 ³	562.3	59274.041806
HD 59498	B5IVe	4.59	91.9	0.105	94.7	875.5	59272.093981
OY Hya	B5Ve	4.53	150.8	0.495	337.7	304.6	59227.311725
CK Cir	B2Vne	3.14	700.6	1.045	295.9	670.4	59418.068738
CU Cir	B3Vne	0.68	86.3	0.13	264.0	664.2	59418.080498
CW Cir	B0.5Vne	4.83	655.1	0.732	162.5	894.9	59418.091181
HD 139431	B2Vne	4.1	37.5	0.057	292.5	658.0	59419.073831
66 Oph	B2Ve	2.16	10.4	0.051	211.0 ³	203.1	59391.442627
QR Vul	B3Ve	2.7	70.1	0.393	192.3	178.4	59393.509965
V2120 Cyg	B2Ve	2.6	72.5	0.083	171.2	874.0	59389.517546

NOTE—¹ Given in the 832 nm filter; ² Distance from *Gaia* DR3 results in [Bailer-Jones et al. \(2021\)](#); ³ 180° ambiguity in the fit; ⁴ Given in the 562 nm filter

ported in Table 2. For close separations (<100 mas), we found six sources. For two (66 Oph and FV CMa), the companions were detected in our speckle imaging. The other companions were to 60 Cyg (HIP 103732), a known multiple star from [Koubský et al. \(2000\)](#), with the secondary identified as a hot subdwarf from ultraviolet spectra in [\(Wang et al. 2017\)](#). The reported companion here is the same, but detected via interferometry by [Klement et al. \(2022\)](#). A companion to V4024 Sgr (γ Cas variable) was identified, that is marked as a potential binary in [Mason et al. \(2022\)](#), based on lunar occultation observations of [Evans & Edwards \(1981\)](#). However, on further inspection, [Wang et al. \(2018\)](#) using spectroscopy found no companion, and suggested that previous changes reported in the cross-correlation function are due to spectral features of the Be star, and not due to a companion. We therefore discard the notion that V4024 Sgr is a binary. Interferometric observations of μ Cen by [Rizzuto et al. \(2013\)](#) detect a companion at $0.1''$, and it is marked as a multiple in our study. This companion is at the speckle detection limits, and is not identified in our data. QV Tel ([Frost et al. 2022](#)) has a companion at 1 mas detected via interferometric imaging, and predicted via spectroscopy ([Bodensteiner et al. 2020b](#)). Four other companions are within our detection limits ($\lesssim 1.2''$), and all (companions to QR Vul, OY Hya, CK Cir), but one (FV CMa) are found in previous speckle imaging with similar separations and Δm . FV CMa has a closer companion detected previously in speckle imaging by [Hartkopf et al. \(2012\)](#) and our images, but this companion (found by [Oudmaijer & Parr \(2010\)](#))

(2010) at a separation of $0.7''$, $\Delta m \sim 6$) is undetected from the speckle analysis, possibly due to the combination of the secondary's brightness, and the tertiary being close to the detection limit (and also in the infrared). It is reported as a triple in Table 3.

We now inspect the remaining 20 stars for possible companions (all at separations greater than 2 arcsec), which were detected based on classical seeing-limited imaging. To estimate the likelihood of the companions being related, we compare the *Gaia* DR3 reported astrometry (parallax, proper motions), and the chance alignment probability described in Section 3.1. The binaries are listed in Table 3. For the binaries, we find that μ Cen has a companion (detected in adaptive optics images of [Oudmaijer & Parr 2010](#)) at $4.3''$ with Δm of 6 mag (in K). Given the similarity in astrometry (within 1σ) for the $4.3''$ companion, we consider this as a potential wide triple companion. Although the chance alignment probability of V423 Lac is high (90%), the companion reported in WDS has the same *Gaia* parallaxes and proper motions (less than 1σ difference) as the primary, suggesting that the binary maybe be physical. We therefore consider it as a candidate companion. 60 Cyg also a $\Delta m=4.13$ companion within $2.9''$, which has a low chance alignment probability, which we mark a triple to the inner spectroscopic companion given the similarity in astrometry to the primary. We note that although κ^1 Aps has a reported close binary companion (1470 au) in [Lindroos \(1986\)](#), the system is likely not

Table 2. WDS multiples cross-matches

Name	WDS	Sep.	P.A.	<i>V</i>	Δm	ρ	Probability ¹
	Identifier	($''$)	$^{\circ}$	(mag)	(mag)	(sources/ $''^2$)	(%)
FV CMa ²	07074-2350	0.09	201	5.71	1.99	15	0.01
FV CMa ³	07074-2350	0.7	228	5.7	6.0 ⁵	10	0.43
NV Pup	07183-3644	241.6	102	4.66	0.41	4	100.0
NW Pup	07183-3644	118.9	215	5.07	3.6	4	100.0
<i>o</i> Pup	07481-2556	26.9	197	4.5	8.1	59	100.0
I Hya	09413-2335	51.8	293	4.77	6.19	2	99.08
OY Hya ²	09591-2357	0.5	341	6.15	4.29	1	0.02
μ Cen ³	13496-4228	0.1	80	3.5	3.2	8	0.01
μ Cen ³	13496-4228	4.6	304	3.97	6.09 ⁵	8	13.73
μ Cen	13496-4228	45.5	127	3.46	9.5	10	100.0
V795 Cen	14150-5705	5.3	296	4.83	10.24	36	58.62
V795 Cen	14150-5705	37.8	235	5.03	7.47	36	100.0
V795 Cen	14150-5705	32.3	165	5.03	5.97	36	100.0
CK Cir	14395-6812	16.2	256	6.76	6.08	25	99.67
CK Cir ²	14395-6812	1.1	295	6.91	3.15	25	2.61
κ^1 Aps ⁴	15315-7323	27.4	255	5.49	5.78	6	98.04
MQ TrA	16037-6030	53.0	179	7.13	0.98	14	100.0
66 Oph ²	18003+0422	0.05	216	5.0	1.5	4	0.0
QV Tel ³	18171-5601	0.02	137	5.9	0.3	5	0.0
λ Pav	18522-6211	60.6	205	4.22	8.18	4	100.0
V4024 Sgr ⁴	19083-1917	<0.1	-1	5.5	3.6	7	0.01
QR Vul ²	20153+2536	0.4	190	4.8	2.75	11	0.15
QR Vul	20153+2536	115.7	83	4.8	4.9	11	100.0
V2120 Cyg	20255+5441	47.3	147	7.25	3.95	10	100.0
V2120 Cyg	20255+5441	50.3	204	7.25	4.55	10	100.0
60 Cyg ³	21012+4609	2.9	159	5.4	4.13	22	14.91
60 Cyg ³	21012+4609	0.04	14	6.7	--	22	0.0
ϵ Cap	21371-1928	65.8	46	4.49	5.62	1	97.71
ϵ Cap	21371-1928	62.7	164	4.49	9.61	1	96.76
V423 Lac ³	22558+4334	28.8	167	8.0	1.54	3	88.6

NOTE—¹ Refers to the chance alignment probability. ²Identified in speckle imaging ³Added as archival multiple ⁴Rejected as binary, see Section 3.2.1. ⁵Reported in the *K*-band.

physical given the significant differences in parallax and properties, but a chance superimposition instead. The remaining sources are much farther out with very high chance alignment probabilities, and have *Gaia* astrometry more than 3σ different from the primary suggesting a chance alignment and are hence rejected.

Overall, based on the WDS compilation, we catalog companions from the WDS catalog (given in Table 3) based on archival interferometric imaging for 60 Cyg (added in Table 4 as detected spectroscopically as well), QV Tel, μ Cen, archival infrared AO imaging

for FV CMa, μ Cen, and classical seeing-limited imaging for V423 Lac and 60 Cyg.

3.2.2. Spectroscopic counterparts

For each source, we searched for possible spectroscopic counterparts. To do so, we used the listed SIMBAD database object types, where we found 5 classified as potential spectroscopic binary candidates (χ Oph, π Aqr, CX Dra, EW Lac, HD 134401), with the references tabulated in Table 4. The first three are catalogued in the survey of Pourbaix et al. (2004). The remaining two are

Table 3. Properties of multiples reported based on archival observations listed in WDS

Name	Sp. type	Δm^1	Sep. (mag)	Sep. (au)	P.A. ($''$)	Dist. ² (pc)
FV CMa ⁵	B2Vnne	6.0 ³	587.6	0.7	228	734.52
μ Cen	B2Vnpe	3.2	14.0	0.1	80	139.89
μ Cen	B2Vnpe	6.09 ³	643.5	4.6	304	139.89
QV Tel	B3IIIipe	0.3	0.44	0.001	137	364
60 Cyg ⁴	B1Ve	4.13	1087.7	2.9	159	375.06
V2155 Cyg ^{6,*}	B1Ve	--	--	--	--	1104.5
V423 Lac*	B3Vne	1.54	16831.3	28.8	167	584.42

NOTE—¹ Reported from WDS catalog in V except where references mentioned; ²Distance from *Gaia* DR3 results of Bailer-Jones et al. (2021) ³ K -band from Oudmaijer & Parr (2010) ⁴ Potential triple to inner spectroscopic companion; ⁵Triple, secondary is detected in speckle imaging at 65 au. ⁶ Candidate binary based on *Gaia* RUWE parameter. * denotes candidate binaries.

listed from the *Gaia* non-single stars catalog identified using *Gaia* multi-epoch radial velocity spectra combined with astrometry, and are marked as candidate binaries. We also cross-matched with the compilation of bright Be binaries from Bodensteiner et al. (2020a) with 11 cross-matches, where in addition to the previously identified binaries (and in some cases, non-detections), we report one possible binary subdwarf candidate, o Pup (Koubský et al. 2012). We found one companion in the catalog of Rivinius et al. (2006), ϵ Cap with a period of 128.5 days. κ^1 Aps is a spectroscopic binary, with sdB companion reported in Wang et al. (2023). We found no new companions when comparing with the LAMOST spectroscopic double lined survey (Zheng et al. 2023).

Therefore, in addition to our 11 speckle companions, we identify seven companions in the WDS catalog, and nine spectroscopic companions from the literature. A further candidate binary is added based on *Gaia* astrometry (V2155 Cyg; see Section 3.2.3). Of these multiples, three are triples (μ Cen, 60 Cyg, FV CMa). These literature companions are listed in Tables 3 and 4. The catalog of WDS companions, including the determination of the companion parameters is presented in Table 2.

3.2.3. *Gaia* multiplicity indicators

Gaia provides multiple parameters to identify potential multiples based on astrometry (besides the spectroscopic candidates identified in Section 3.2.1). Here, we consider two primary criteria, which are listed below—

Table 4. Properties of multiples detected based on archival spectroscopic data

Name	Sp. type	Period (days)	q	Ref.	Dist. ¹ (pc)
o Pup	B1IVnne	28.9	--	7	354.50
HD 134401*	B2Vne	1113.34	--	5	968.76
κ^1 Aps	B2Vnpe	192.1	0.14	12	
χ Oph	B2Vne	138.8	--	2	153.00
CX Dra	B2.5Ve	6.70	0.23	4	351.23
60 Cyg ⁸	B1Ve	146.6	0.13	9, 10	375.06
ϵ Cap	B3Vpe	128.5	--	11	270.56
π Aqr	B1Ve	84.1	0.16	3	333.05
EW Lac*	B3IVpe	4.56	0.99	5, 6	285.61

NOTE—¹ Distance from Bailer-Jones et al. (2021); ² Abt (2005); ³ Bjorkman et al. (2002); ⁴ Richards et al. (2000); ⁵ Gaia Collaboration et al. (2023); ⁶ Candidate in Klement et al. (2024) based on SED ⁷ Koubský et al. (2012); ⁸ Detected both in spectroscopy and interferometry; ⁹ Koubský et al. (2000); ¹⁰ Klement et al. (2022); ¹¹ Rivinius et al. (2006); ¹² Wang et al. (2023). * denotes candidate binaries.

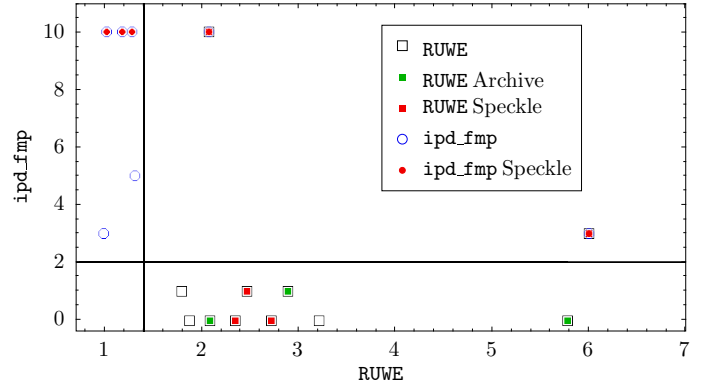


Figure 8. Candidate binaries meeting either of the *Gaia* binary indicators. RUWE candidates are shown by black squares, with the cut-off of 1.4 marked, and ipd_frac_mp candidates are shown as blue circles where the cut-off (>2) is shown by a solid line. Detected archival, or speckle companions are shown by filled green and red markers respectively. For visual purposes, the maximum ipd_frac_mp value was set to 10, and the RUWE value to 6.

1. The Gaia Renormalized Unit Weight Error (termed RUWE) is the root of the normalized χ^2 of the astrometric fit to along-scan observations. For candidates with multiple companions, this values is expected to be >1.4 (Lindegren et al. 2021).

This parameter can detect companions between $0.04\text{--}0.7''$ (Dodd et al. 2024).

2. The percentage of windows used for astrometric processing that contain more than one peak is sensitive (the *Gaia ipd_frac_multi_peak* parameter) to close binaries, as it produces multiple peaks in some scan directions. Following Tokovinin (2023), we identify candidates having values greater than 2.

In Fig. 8, we compare the first two indicators provided from the *Gaia* parameters. Here, we find that all stars meeting both criteria are detected as binaries in our sample. However, three stars meeting the RUWE parameter (NV Pup; V2155 Cyg, and f Car) were not identified as binaries in our sample. NV Pup was identified as a potential binary (with a separation of $240''$ given in Table 2) in our sample. However, if the high RUWE is caused by a closer companion if present, we do not find any literature identification as a binary for NV Pup, which is a known γ Cas variable. Similarly, f Car is also a variable star (Ruban et al. 2006). Variability is expected to affect the measured RUWE parameter (Belokurov et al. 2020). Additionally, although Fitton et al. (2022) have reported that extended discs of asymptotic giant branch stars might inflate the RUWE parameter, this is not strictly applicable to Be stars, which have smaller discs. However, even adopting a stricter cut-off $\text{RUWE} > 2$, we still have V2155 Cyg as a binary which remains unidentified in our sample. No literature information was found on its binary status. We mark it as a potential binary. Two stars (z Pup, and HD 55135) are found as a potential binary from the peak fraction, but no literature information could be found on their status. These are much lower than the cut-off suggested by other works (for e.g. Cifuentes et al. 2025 suggest $\text{ipd_fmp} > 30$, although CU Cir has a ipd_fmp of 3, but an $\text{RUWE} > 10$). We therefore, suggest a cut-off in $\text{ipd_fmp} > 10$ for Be stars.

We add, from comparison with *Gaia* binary indicators one potential binary V2155 Cyg (but without binary parameters). The remaining candidates with stringent cut-offs ($\text{ipd_fmp} > 10$; or $\text{RUWE} > 2$) are all detected in either speckle or in the WDS catalog. We suggest that for Be disc bearing stars, more conservative cut-offs are necessary to identify binarity.

4. DISCUSSION

4.1. Multiplicity fraction

In our study, we observed 76 Classical Be stars within 1000 pc (Appendix A) using speckle imaging covering a separation range of $20 \text{ mas} - 1.2''$, reaching $\Delta m < 6 \text{ mag}$.

We found 11 companions, six of which were previously unreported in the literature. We then combined our datasets with archival literature, imaging, and *Gaia* binary indicators. We found another 16 companions, three of which were triples. The total number of multiples in our sample is 24, resulting in an observed multiplicity fraction of $32 \pm 5\%$ (error accounting for candidate multiples), but for our speckle candidates only (i.e. with separation range of $20 \text{ mas} - 1.2''$) is $\sim 15\%$. No corrections were made for potentially missing companions based on our detection limitations. Compared to the literature, our fraction is similar, but covers a vaster breadth in separation ranges. A comparison to literature derived multiplicity fractions are given in Table 5.

Following the Clopper-Pearson method described in Kalari et al. (2024), we can rule out a multiplicity fraction greater than 47% within our speckle detection limits (see Fig. 7), at the 3σ confidence level. For speckle only companions, this falls to 27%. Our speckle multiple fraction is on the lower end of multiplicity studies for Be stars. From speckle interferometry Hutter et al. (2021) found a 45% multiplicity fraction for nearby bright Be stars, Oudmaijer & Parr (2010) reports a Be binary fraction of 30% from AO imaging, and Dodd et al. (2024) show a 29% binary fraction from *Gaia* proper motion anomaly study. Our values are similar to limited speckle surveys (Mason et al. 1997 with separations greater than $0.03''$; or Guerrero et al. 2025 with separations between $0.09\text{--}0.33''$); or the literature spectroscopic study of Bodensteiner et al. (2020a) which probes a smaller separation range than in this study. *It is not apparent if the different separation ranges have different multiplicity fractions due to physical effects, or the observed multiplicity fractions at these different separation ranges are purely due to the observational differences between speckle imaging, interferometry, and spectroscopy.* The speckle images are more sensitive to close binaries than literature imaging and *Gaia* surveys (but not always in Δm). Combining archival imaging observations to encompass binaries at larger separations, our multiplicity fraction still remains low ($\sim 24\%$), indicating that a simple lack of candidates beyond our detection limits is not the reason for the low multiplicity fraction observed for our targets. Including spectroscopic companions, our multiplicity fraction is around $\sim 32\%$, similar to recent literature studies.

We consider the observed multiplicity fraction a combination of multiple effects. It is most likely that our sample, with a mean distance of around 580 pc is further than most previous studies. In our case, the angu-

Table 5. Literature Be star multiplicity fractions

Method	Scope ¹	Sp. type	Fraction	Size	Reference
Spectroscopy ²	$B < 5$ mag	B2–B5IV	25%	42	Abt & Levy (1978)
Imaging ³ (with select spectra)	$V < 6.5$ mag	B2–B7	28%	80	Abt & Cardona (1984)
Speckle ⁴	$V < 6.5$ mag	B1–B8	10%	48	Mason et al. (1997)
AO imaging ⁵	$K < 7$ mag	B0–B9	30%	39	Oudmaijer & Parr (2010)
Spectroscopy ⁶	$V < 12$ mag	B0-B1.5	10%	287	Bodensteiner et al. (2020a)
Interferometry	$V < 5$	B0-B9	45%	31	Hutter et al. (2021)
<i>Gaia</i> ⁷	--	B0-B9	29%	123	Dodd et al. (2024)
Speckle ⁸	$V < 11$	O8-B9	26%	46	Guerrero et al. (2025)
Speckle ⁹	< 1000 pc	B0-B5	14%	76	This work
Speckle, and archival ¹⁰	< 1000 pc	B0-B5	32%	76	This work

NOTE—¹Magnitude or distance limit; ²Around 10 epochs per star, resolution of 5 km s^{-1} ; ³ from Bright star catalog; ⁴Separations 0.035–1.5'' and $\Delta m < 3.0$; ⁵Separations of 0.1–8'', $\Delta m < 10$ mag; ⁶Literature analysis; ⁷Combination of *Gaia* PMa; and RUWE parameter, quoted separations of 0.02''–1.1''; ⁸ Separations of 0.06–9.7'', with $\Delta m < 4.8$ mag ⁹0.020–1.2'', with $\Delta m < 2$ –6 mag; ¹⁰ Archival imaging and spectroscopic observations along with speckle imaging

lar resolution achieved probes a smaller physical separation range in au (i.e. spectroscopy/interferometry/*Gaia* probes closer separation ranges; while imaging finds companions further out). C.f. a median distance of 280 pc in Dodd et al. (2024); a limit of $K < 6$ mag in Oudmaijer & Parr (2010); $V < 5$ mag in Hutter et al. (2021) to our mean distance of 580 pc, which suggests that those studies probe closer multiples (~ 5 au) for the median distance. In addition, our limited separation range, and detection limit means that candidates even if present (for e.g. see FV CMa) may not be detected given our observational limitations.

4.1.1. Comparison with Proper Motion Anomaly Be binaries

We compare our catalog to the binaries detected in Dodd et al. (2024). In that paper, Dodd et al. (2024) used a combination of either *Hipparcos* and *Gaia* DR2 or DR3 astrometry to compute the proper motion anomaly (PMa; Kervella et al. 2021). Essentially the method compares the long-term proper motion vector (measured over the almost 25 years elapsed between the *Hipparcos* and *Gaia* DR3 data acquisition for example) with the short-term proper motion as measured by either *Gaia* or *Hipparcos*. For a single star, the proper motions would be similar, in case of a binary system, a change in proper motion (the PMa) indicates orbital motion in an otherwise unresolved binary system. Dodd et al. (2024) determine that the *Hipparcos*–*Gaia* DR3 PMa is sensitive to binary systems with separations from about 20 mas to the spatial resolution of *Gaia*, 0.7 arcsec. They also found that a magnitude difference of at least 4 can

be probed using the method, with as proviso that the smaller the magnitude difference, the smaller any change in motion of the photo-center and thus PMa will be.

Here we concentrate on the *Hipparcos*–*Gaia* DR3 PMa as that has the best separation overlap with our speckle data. Ten of the 11 binary systems in Table 1 have a listing in the PMa catalogue by Kervella et al. (2021). Seven (70%) of these are identified as a binary system based on their large PMa. Three objects have a PMa signal-to-noise ratio less than 3, and are thus not recognized as a binary. It may be useful to point out that of these three, CW Cir has a separation of 0.732 arcsec in our speckle imaging, and this is at the higher separation limit probed by the *Hipparcos*–*Gaia* DR3 PMa, whereas HD 56039 and CU Cir have very small magnitude differences of 0.84 and 0.68 mag. respectively. This will have drastically reduced the PMa values. Hence, the detection statistics of the speckle binary systems are consistent with the PMa.

Of the 65 objects that are not found as binary in our data, 53 are present in the catalog Kervella et al. (2021), of which 9 (17%) have a significant PMa. As the PMa is capable of identifying binary systems with magnitude differences larger than the speckle imaging Δm limit, we suspect that these systems have too faint companions to be detected in the speckle data. We suggest that further high-resolution imaging, or spectroscopic follow-up is necessary to verify the Be binaries identified through *Gaia* PMa values where possible.

4.1.2. Limitations

Although the multiplicity fraction of early-type stars is very high (approaching 100%), the vast majority are close-in, detected at less than 10 mas (Frost et al. 2025). In that paper, 72% of B stars identified by interferometry have binaries, however, fewer 20% of binaries detected would have been detected by speckle imaging as they are extremely close (< 25 mas). Future follow-up observations in the spectroscopic and interferometric space are necessary to populate the parameter space not covered in this study.

4.2. Nature of detected companions

We plot the separation range of all companions in Fig. 9, and describe the characteristics in Table 6. The build-up of close-in companions are due to the spectroscopic companions, and the interferometrically identified binary of QV Tel. For spectroscopic binaries, we estimated the separation based on the period, and the mass of both components from the spectral type following Pecaut & Mamajek (2013). Where the companion spectral type was unknown, we assumed a mass ratio of 0.5.

The speckle companions and archival imaging companions have separations > 10 au. Currently, this result is not in agreement with a flat distribution (Öpik's law) noted in the literature (Offner et al. 2023). There is a build-up of close-in binaries identified spectroscopically, and a lack of binaries beyond this range. We speculate that this result could be a natural consequence of Be star formation via binary interaction, where a close-in companion is necessary to form the Be star (Bodensteiner et al. 2020a; Dodd et al. 2024). However, there is an important caveat. At these distances ($>$ few au), we are constrained by the detection limits of our survey, and the additional literature data. For example, we identify few binaries between $> 2,000$ – $10,000$ au, which we consider a result of the instrumental field of view. Similarly, for the speckle separation range (between roughly few au–few 100s of au depending on the distance), the probability to detect companions with $q < 0.8$ is significantly lower when adopting the period and mass ratio distributions of B stars. Therefore, future dedicated spectroscopic studies, combined with analysis of available astrometric data can help populate further any multiples beyond these detection limits, and confirm if Be stars conform to Öpik's law for companion separation.

For objects with sufficient information to enable companion analysis, we list the nature of the secondary companion, and if known, the orbital period in Table 6. From this we can see that the majority of the speckle companions are early-type main-sequence stars, with exception of OY Hya. For spectroscopically identified close

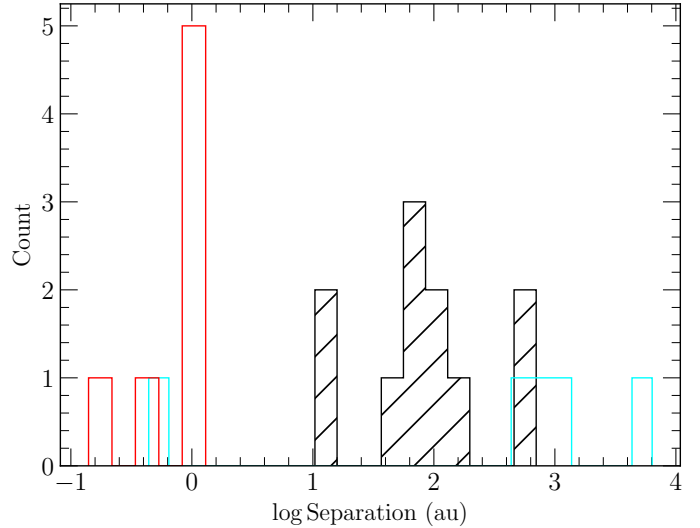


Figure 9. Histogram of separations of known companions. No candidates are included. Black bars represent companions identified in speckle imaging, whereas cyan and red bars are literature imaging and spectroscopic companions respectively. The cyan bar at separation less than 1 au is the interferometric binary identified in QV Tel. The information presented is given in tabular form in tables 1, 3, and 4.

binaries, there are potentially few main-sequence targets, for example π Aqr and CX Dra. Following Bodensteiner et al. (2020a), similar mass main-sequence companions close enough to interact are not expected to be found for Be stars for the binary evolutionary scenario. They discuss the case of π Aqr, and discard it as the companion is not massive enough. Similarly, we also can discard CX Dra as a comparison to their hypothesis, but the candidate companion to EW Lac identified in Gaia Collaboration et al. (2023) is predicted to be a near equal-mass close-in companion and deserves further follow-up.

4.3. Formation mechanisms

In this paper, we attempted to constrain the multiplicity fraction of CBes across the few au to few thousand au range. For most of our targets, we cannot rule out close binaries, and thereby Be binaries formed via mass transfer leading to an evolved close-in companions (e.g. see Rivinius & Klement 2024). However, if we consider the assumption that all our stars have a close-in undetected companion, some will be triple or higher order multiple systems when combined with the companions presented here (see Moe & Di Stefano 2017). As an e.g., 60 Cyg has a close-in evolved sdB companion and a wider companion, or FV CMa, μ Cen have two wider companions (> 50 au). In such hierarchical triple systems with a more distant outer body, the Kozai-Lidov mechanism

Table 6. Primary and companion characteristics

Name	Primary	Secondary	Period
	Sp. type	Sp. type	
Spectroscopy			
κ^1 Aps ⁵	B2Vnpe	sd0	192.1d
CX Dra ²	B2.5V	F5III	6.7d
60 Cyg ⁴	B1Ve	sd0	146.6d
π Aqr ¹	B1Ve	A-FV*	84.1d
EW Lac ³	B3IVpe	B3-B4*	4.6d
Speckle imaging			
FV CMa	B2Vnne	B8V ⁷	162 yr ⁸
OY Hya	B5Ve	G ⁷	812 yr ⁸
66 Oph ⁶	B2V	B8V	64.2 yr
QR Vul	B3Ve	A3V ⁷	217 yr ⁸
V2120 Cyg	B2V	B6V ⁷	235.4 yr ⁸

NOTE—¹Naze et al. (2017), secondary nature not well constrained; ²Berdyugin et al. (2002), Richards et al. (1999); ³ based on *Gaia* spectroscopy, SED shows downturn. Mass based on ratio; ⁴Wang et al. 2017; ⁵Wang et al. 2023; ⁶Hutter et al. 2021 orbital and secondary determination; ⁷Approximate, based on stellar mass tracks assuming same age as primary; ⁸ Lower limit estimate based on orbital separation, and mass of system assuming no eccentricity

(Naoz 2016) and its interaction with the circumstellar disc must be considered, assuming the inclination of the system meets the criteria (inclination between the two bodies differ by more than 39°).

In such circumstances, the triple systems are predicted to lead to oscillation driven outbursts (Martin & Franchini 2019), or changes in the emission line profiles due to disc tearing (Suffak et al. 2025). Further study of such hierarchical systems, in particular determining the orbital parameters and inclination may help understand the impact of the Kozai-Lidov mechanism on observables in Be stars.

5. CONCLUSIONS

In this study we observed via speckle imaging 76 known Classical Be stars, ranging from B0-B5 spectral subtypes, located within $\lesssim 1$ kpc from us. The angular separation range probed is between ~ 5 au–1000 au de-

pending on the distance of the source. Our main results are—

1. Identification of 11 companions, of which 6 have no previous literature. Complementary literature search revealed another 16 companions (incl. three triples) indicating 24 multiples.
2. We rule out a multiplicity fraction greater than 27% within the detection limits for speckle interferometry (between 20 mas–0.1'' to ~ 1 –5 mag, and 0.1''–1.0'' reaching $\Delta m < 5$ –6 mag). Combined with literature, we rule out a multiplicity fraction $> 47\%$, but without the homogeneity afforded by the speckle survey.

We thank the anonymous referee for useful comments which helped improve the manuscript. V. M. K. thanks A. Tokovinin for useful comments regarding QV Tel, and S. Deveny for providing the intermediate data reduction products for HD 56039. This research has made use of the SIMBAD and VIZIER databases, operated at CDS, Strasbourg, France. This research made use of the STARLINK software, TOPCAT. This work has made use of the BeSS database, operated at LESIA, Observatoire de Meudon, France: <http://basebe.obspm.fr>. Observations in the paper made use of the High-Resolution Imaging instruments 'Alopeke and Zorro. 'Alopeke and Zorro were funded by the NASA Exoplanet Exploration Program and built at the NASA Ames Research Center by Steve B. Howell, Nic Scott, Elliott P. Horch, and Emmett Quigley. 'Alopeke and Zorro are mounted on the Gemini North and South telescopes of the international Gemini Observatory, a program of NSF NOIRLab, which is managed by the Association of Universities for Research in Astronomy (AURA) under a cooperative agreement with the U.S. National Science Foundation. on behalf of the Gemini partnership: the U.S. National Science Foundation (United States), National Research Council (Canada), Agencia Nacional de Investigación y Desarrollo (Chile), Ministerio de Ciencia, Tecnología e Innovación (Argentina), Ministério da Ciência, Tecnologia, Inovações e Comunicações (Brazil), and Korea Astronomy and Space Science Institute (Republic of Korea).

Facilities: Gemini-North ('Alopeke); Gemini-South (Zorro)

APPENDIX

A. CLASSICAL BE STARS OBSERVED.

Table 1. Classical Be stars observed.

Name	Sp. type	Right Ascension ¹ (hh:mm:ss)	Declination ¹ (dd:mm:ss)	V (mag)	HD ID	Airmass	MJD	0.1'' Limit (Δm)	1'' Limit (Δm)
HD 52812	B3Ve	07:01:33.61	-27:13:22.60	6.93	52812	1.0	59228.187731	4.8	8.7
19 Mon	B1Ve	07:02:54.78	-04:14:21.24	5.0	52918	1.16	59253.393218	5.3	8.2
HD 54086	B5IIIe	07:06:52.31	-14:41:54.34	9.19	54086	1.04	59228.19213	4.8	8.7
FV CMa	B2Vnne	07:07:22.59	-23:50:26.59	5.83	54309	1.09	59227.251019	4.4	8.3
HD 55135	B2.5Ve	07:11:20.85	-10:25:43.78	7.32	55135	1.1	59228.225289	4.9	8.8
HD 56039	B5Ve	07:14:59.91	-11:52:13.47	8.28	56039	1.06	59274.039618	4.9	8.4
NV Pup	B2Ve	07:18:18.39	-36:44:02.23	4.67	57150	1.02	59273.089734	4.8	8.3
NW Pup	B2IVnne	07:18:38.19	-36:44:33.85	5.11	57219	1.03	59273.102512	5.1	8.0
OT Gem	B2Ve	07:24:27.65	+15:31:01.91	6.41	58050	1.03	59252.395544	4.5	8.5
HD 59498	B5IVe	07:29:22.78	-21:52:09.18	7.79	59498	1.02	59272.092523	4.6	8.1
V373 Pup	B2Vne	07:29:27.97	-21:51:31.03	7.73	59497	1.03	59272.10544	4.7	8.0
z Pup	B3Vne	07:33:51.04	-36:20:18.21	5.44	60606	1.01	59271.09316	4.1	8.5
o Pup	B1IVnne	07:48:05.17	-25:56:13.81	4.49	63462	1.01	59228.221667	4.6	8.1
BT CMi	B2Vne	07:57:03.99	+02:57:03.04	7.77	65079	1.21	59228.23456	4.4	7.4
V374 Car	B2IVnpe	07:58:50.55	-60:49:28.06	5.81	66194	1.18	59228.258542	4.5	8.8
HD 68468	B3npshe	08:12:00.39	-14:10:08.37	8.3	68468	1.04	59228.239074	4.3	9.1
r Pup	B1.5IIIe	08:13:29.52	-35:53:58.27	4.77	68980	1.01	59228.249641	4.7	8.6
HD 69168	B2Ve	08:13:45.65	-46:34:43.27	6.48	69168	1.08	59271.157072	5.0	8.3
HD 69404	B2Vnne	08:14:51.24	-46:29:09.21	6.44	69404	1.05	59228.254097	4.5	8.3
f Car	B3Vne	08:46:42.55	-56:46:11.19	4.49	75311	1.14	59227.293356	4.7	8.8
HD 76985	B5Vne	08:56:47.14	-59:31:12.01	9.05	76985	1.15	59227.282072	4.9	8.2
IU Vel	B2.5Vne	09:00:22.26	-43:10:26.36	6.08	77320	1.03	59227.271192	4.9	8.6
E Car	B2IVe	09:05:38.38	-70:32:18.60	4.65	78764	1.32	59227.288171	4.8	8.3
I Hya	B5Ve	09:41:17.01	-23:35:29.45	4.76	83953	1.01	59227.264722	4.5	7.6
V485 Car	B3IIIPshe	09:41:37.30	-68:30:17.96	7.1	84375	1.27	59227.298924	5.1	8.4
HD 85083	B5IIIe	09:47:34.01	-58:11:16.70	8.27	85083	1.13	59227.304352	5.2	8.5
OY Hya	B5Ve	09:59:06.30	-23:57:02.77	6.25	86612	1.01	59227.310995	4.3	7.7
HD 89884	B5IIIe	10:21:59.40	-18:02:04.13	7.13	89884	1.03	59274.208252	5.0	7.7
V353 Car	B2Ve	11:10:02.34	-60:05:42.49	7.74	97151	1.16	58924.201817	4.0	8.3
HD 103574	B2Ve	11:55:21.66	-63:42:12.79	7.98	103574	1.2	58924.21559	4.5	8.2
DK Cru	B2IVnne	12:14:01.77	-59:23:48.83	8.81	106309	1.15	58924.25206	4.6	8.1
39 Cru	B5IIIe	12:41:56.57	-59:41:08.95	4.94	110335	1.15	58923.253032	5.1	8.2
GP Vir	B3e	13:35:43.32	-06:09:22.05	8.01	118246	1.09	58924.283044	5.0	8.3
μ Cen	B2Vnpe	13:49:36.99	-42:28:25.43	3.43	120324	1.03	58923.310556	4.5	8.0
V774 Cen	B3Vne	13:53:28.23	-39:03:25.93	7.61	120958	1.02	58923.318819	4.9	7.7
V795 Cen	B4Vne	14:14:57.14	-57:05:10.05	5.07	124367	1.18	59418.026354	4.7	8.4

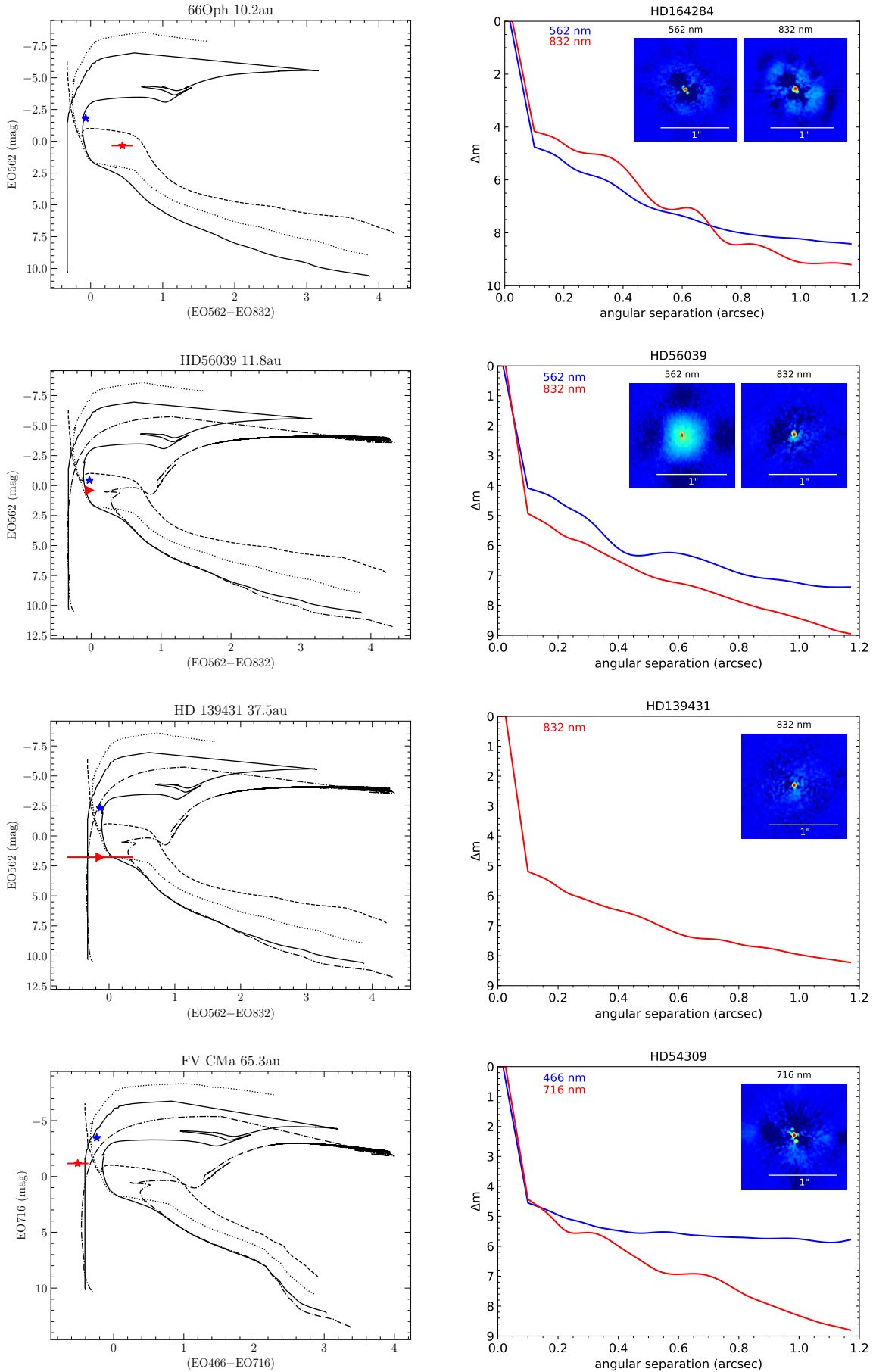
B. INDIVIDUAL OBJECTS

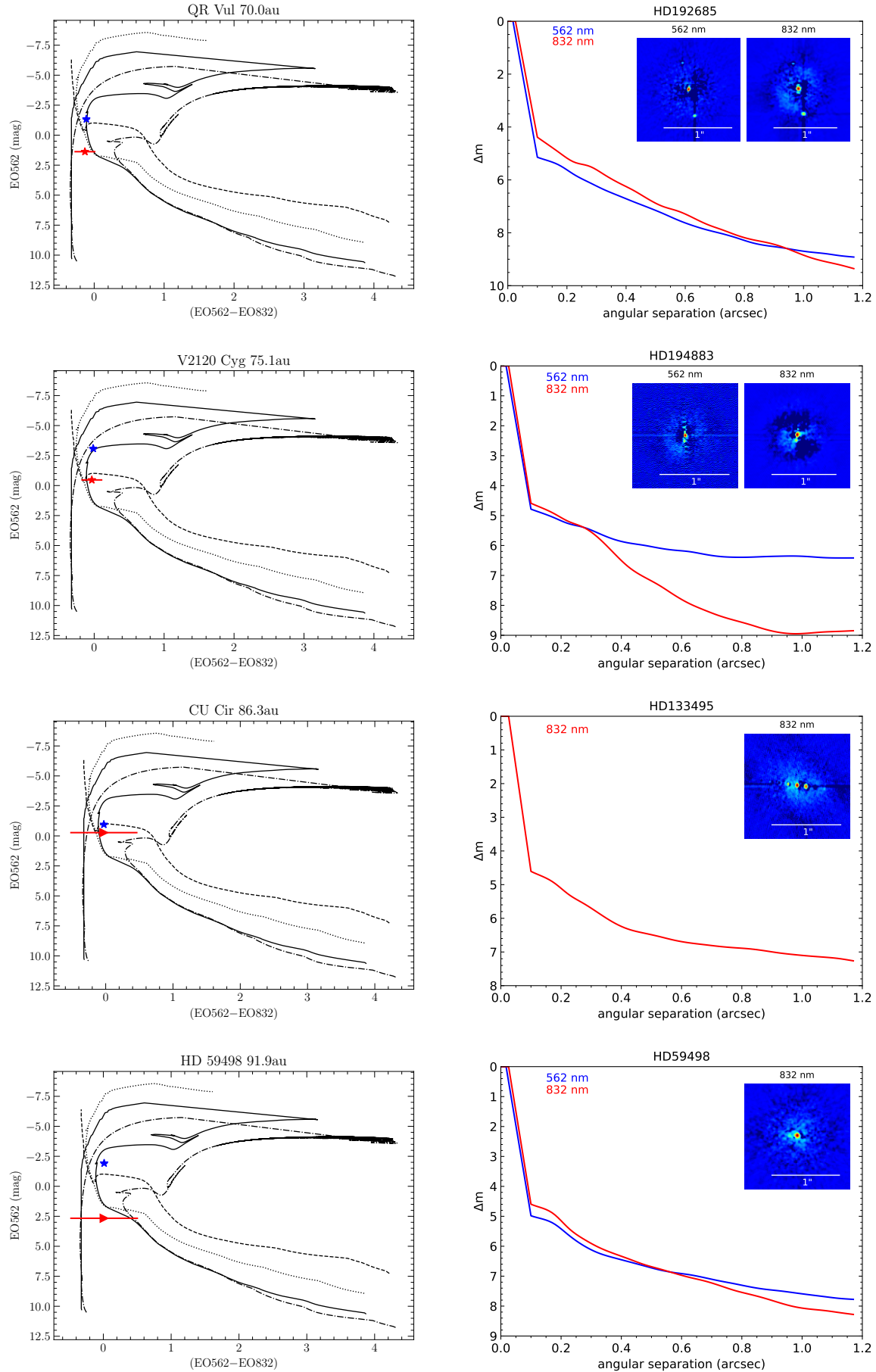
B.1. *Notes on individual objects*

66 Oph (HD 164284, HIP 88149, HR 6712, WDS 18003 +0422) is a known binary star previously

CK Cir	B2Vne	14:39:31.66	-68:12:12.19	6.93	128293	1.36	59418.06728	4.9	8.1		
V1012 Cen	B3Vne	14:40:05.48	-59:55:52.88	9.08	128588	1.15	58924.322361	5.1	8.6		
CU Cir	B3Vne	15:07:30.08	-60:46:36.53	8.54	133495	1.25	59418.077581	4.6	7.1		
HD 134401	B2Vne	15:13:12.16	-65:58:09.03	8.98	134401	1.23	58924.356157	5.0	7.4		
CW Cir	B0.5Vne	15:15:16.17	-58:10:22.37	8.19	134958	1.23	59418.088993	5.1	7.6		
κ^1 Aps	B2Vnpe	15:31:30.82	-73:23:22.53	5.49	137387	1.37	58924.360185	3.8	7.6		
HD 139431	B2Vne	15:39:45.65	-42:46:02.71	7.34	139431	1.07	59419.070914	5.2	8.0		
V1040 Sco	B2Ve	15:53:55.86	-23:58:41.15	5.4	142184	1.01	59274.403646	5.1	7.6		
MQ TrA	B0Ve	16:03:44.47	-60:29:54.47	7.3	143448	1.16	58923.384861	4.7	8.0		
HD 146463	B3Vnne	16:19:14.23	-54:57:42.12	8.08	146463	1.1	58924.407164	5.3	8.2		
HD 146596	B5IVe	16:19:42.67	-52:46:19.03	7.98	146596	1.09	58924.419375	4.5	8.1		
HD 147302	B2IIIIne	16:24:01.27	-55:27:13.37	7.72	147302	1.11	58923.392731	4.9	7.7		
χ Oph	B2Vne	16:27:01.43	-18:27:22.49	4.43	148184	1.15	59418.129722	4.7	8.9		
V846 Ara	B3Vnpe	16:56:08.84	-50:40:29.25	6.33	152478	1.17	59418.156308	4.9	8.1		
HD 153222	B1IIe	17:00:28.69	-49:15:14.91	8.91	153222	1.18	59418.166481	5.3	7.5		
HD 154218	B3Vne	17:05:42.96	-36:44:25.90	7.57	154218	1.09	59418.149352	5.1	7.6		
HD 156831	B3Vnne	17:20:42.59	-24:16:16.65	8.87	156831	1.06	59419.023056	5.2	8.0		
HD 157099	B3Vne	17:23:13.57	-42:49:45.21	8.83	157099	1.03	58923.420984	4.9	7.6		
66 Oph	B2Ve	18:00:15.80	+04:22:07.02	4.6	164284	1.05	59391.441169	4.2	9.1		
QV Tel	B3IIIipe	18:17:07.53	-56:01:24.07	5.36	167128	1.11	59419.117789	5.8	8.3		
CX Dra	B2.5Ve	18:46:43.09	+52:59:16.66	5.9	174237	1.2	59389.444132	5.0	8.7		
λ Pav	B2Ve	18:52:13.03	-62:11:15.33	4.21	173948	1.34	59418.265035	5.5	8.0		
HD 175863	B4Ve	18:53:44.70	+60:01:04.33	7.03	175863	1.31	59390.467616	4.4	9.0		
V4024 Sgr	B2Ve	19:08:16.70	-19:17:25.03	5.49	178175	1.02	59417.148611	5.2	8.3		
QR Vul	B3Ve	20:15:15.90	+25:35:31.05	4.75	192685	1.0	59393.508507	4.4	8.8		
V2113 Cyg	B1Vnnpe	20:16:48.18	+32:22:47.39	7.16	193009	1.04	59391.544734	3.8	8.5		
V2120 Cyg	B2Ve	20:25:32.81	+54:41:03.12	7.36	194883	1.22	59389.516088	4.6	8.9		
V417 Cep	B1Ve	20:51:09.99	+55:29:19.49	8.33	198895	1.23	59389.528021	4.7	9.2		
60 Cyg	B1Ve	21:01:10.93	+46:09:20.78	5.43	200310	1.12	59390.555012	4.4	9.4		
HD 201522	B0Ve	21:08:29.63	+47:15:25.37	7.9	201522	1.13	59390.562465	4.3	8.5		
6 Cep	B3IVe	21:19:22.22	+64:52:18.68	5.18	203467	1.42	59389.579063	5.1	9.2		
V2155 Cyg	B1Ve	21:24:30.34	+55:22:00.24	7.54	204116	1.23	59391.56265	4.5	9.4		
V432 Cep	B2Vnne	21:36:59.64	+58:08:24.61	8.54	239712	1.27	59389.572373	5.1	9.0		
ϵ Cap	B3Vpe	21:37:04.83	-19:27:57.65	4.55	205637	1.02	59416.285498	5.0	7.7		
HD 206773	B0Vpe	21:42:24.18	+57:44:09.80	6.87	206773	1.28	59389.601678	4.5	7.8		
16 Peg	B3Ve	21:53:03.77	+25:55:30.49	5.08	208057	1.01	59391.588831	4.7	9.3		
UU PsA	B4IVne	22:04:36.77	-26:49:20.50	5.95	209522	1.01	59416.308079	4.1	8.0		
π Aqr	B1Ve	22:25:16.62	+01:22:38.63	4.64	212571	1.34	59419.213032	5.6	7.8		
V423 Lac	B3Vne	22:55:47.06	+43:33:33.43	7.97	216851	1.1	59390.616539	4.3	8.9		
EW Lac	B3IVpe	22:57:04.50	+48:41:02.65	5.43	217050	1.15	59390.608183	4.6	9.2		

NOTE—¹ Given in J2000.





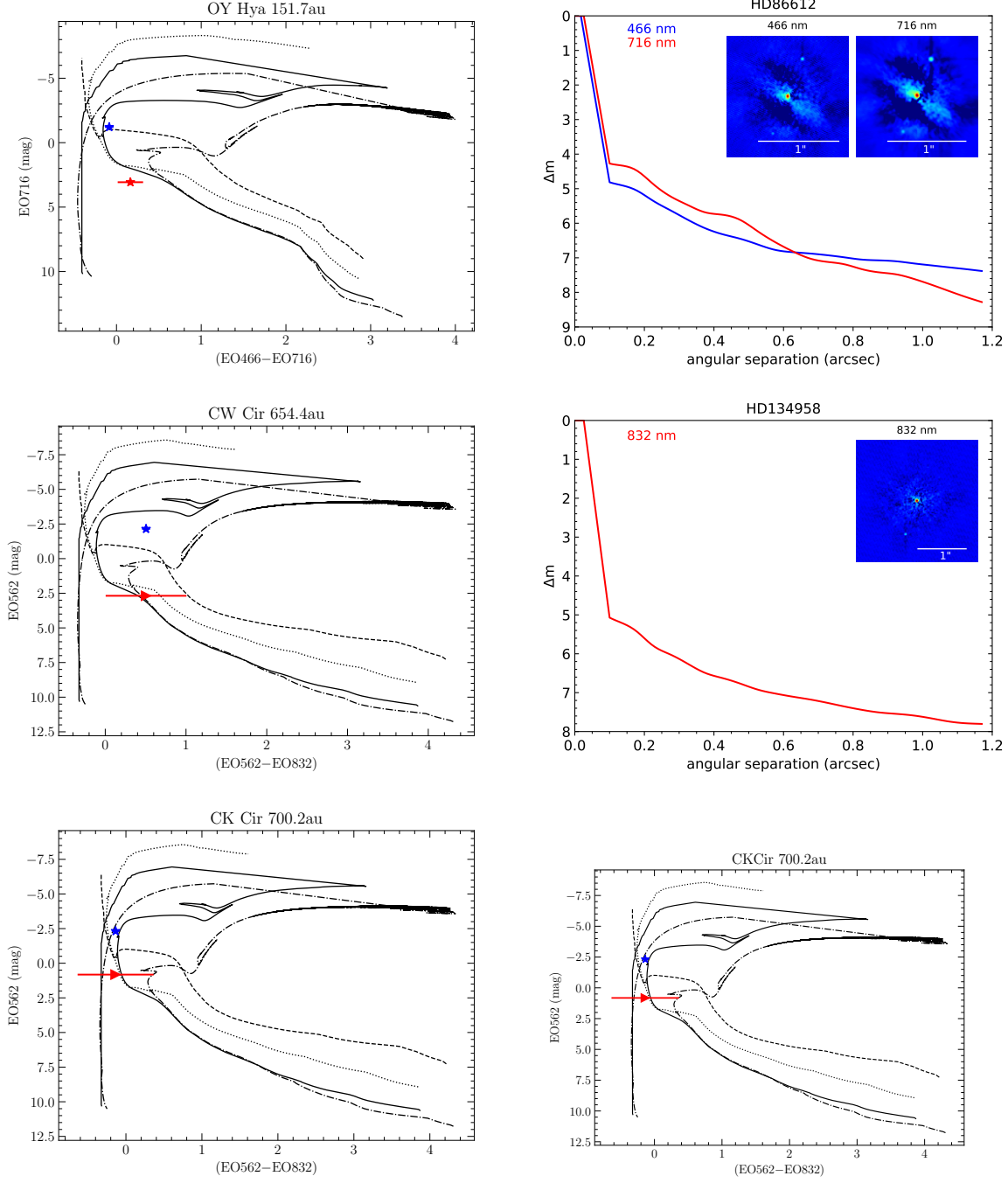


Figure 10. Color-magnitude diagrams (left panel) and reconstructed images and contrast curves (right panel) of multiples detected in two speckle filters. Dotter (2016) isochrones computed in the appropriate filters are plotted for 1, 10, 100 Myrs using dashed, dotted, and solid lines. The dashed dotted line is for 1 Gyr. Stars with magnitude in only one filter are assumed to have the same Δm in the other for plotting purposes, and are marked by a caret with a color error of 0.2 mag.

described in Horch et al. (2020); Hutter et al. (2021), and first identified in Oudmaijer & Parr (2010). Our measurements taken on 26 June 2021 with ‘Alopeke agree within errors with the orbital parameters determined by Hutter et al. (2021). The secondary found by Hutter et al. (2021) was suggested to be a main-sequence B8 spectral type. The period (~ 60 yrs) is sufficiently large to prevent interaction, although the closest approach of the two stars is around 10 au. Based on the Δm from two speckle filters, we compute the position of the secondary on the color-magnitude diagram (CMD). We adopt the solar metallicity MESA (Modules for Experiments in Stellar Astrophysics) Isochrones & Stellar Tracks (MIST) stellar tracks and isochrones (Dotter 2016) and the *Gaia* DR3 extinction Gaia Collaboration et al. (2023) of $A_0=0.186$ mag to estimate the mass and age of the binary components (see Panel(a) of Fig. 10). Since speckle photometry is not absolutely calibrated, we use the *Gaia* DR3 spectrum for absolute flux calibration of the primary. Our results suggest a mass of 8.4 and $3.5 M_\odot$ for the primary and secondary, respectively, assuming a coeval age of 10 Myr to agree with the Hutter et al. (2021) spectral classification of B2 primary and B7/B8 secondary. The companion is visualized in the zoomed-in reconstructed images given in Fig. 11 for 66 Oph, and other companions closer than 0.05”.

It has been recently shown that Be stars are on average brighter than their B-type spectral counterparts in broad G or V -band photometry by ~ 0.5 mag (Radley et al. 2025), but are similar in color. If the Δm of the companions are systematically over-estimated by this amount, this would effect mainly the magnitude and not the color of our sources, and lead to an over-estimate of spectral type by one spectral subclass for companions (Pecaut & Mamajek 2013).

HD 56039 (HIP 35059) was detected as multiple in speckle imaging. The companion to the primary is 11.8 au away assuming the *Gaia* DR3 distance, and has not been previously reported on in the literature. The secondary is detected only at 562 nm, with a small magnitude difference ($\Delta m=0.84$ mag), at very close separation of 21 mas. It is likely that the secondary is beyond the detection limit at 832 nm given its closeness, and based on the detection in the bluer filter likely a main sequence star close to the primary. The power spectrum in both channels, produced as part of the data reduction pipeline is shown in Fig. 12. A blue only detection could also be because of other reasons, such as maybe a single bright blue emission line, or not a Planck spectral energy distribution to be detected. The object should be

re-observed to confirm this detection. Based on the stellar mass, and assuming zero eccentricity, the secondary must have a period of at least 6000 days. Assuming the magnitude limit for the secondary magnitude at 832 nm, it is most likely a B6 star on the main sequence, located too close to the primary. Further observation of this target are essential to confirm the orbital period, and the companion’s properties.

HD 139431 is an early type Be star with a previously unknown companion. Here, we detect a companion within 37.5 au in only EO 832 (observed only in this filter), allowing us to place limits on the secondary. Note the HD 139431 has different spectral classification in the UV (B5Ve) compared to B2Ve/B3Ve from the optical (Skiff 2010), indicating potentially the presence of an evolved hot companion. Interpolating against the Dotter (2016) stellar models and tracks, we compute the primary mass to be $5.6 M_\odot$, with a mass ratio around $q=0.4$, suggesting an early A secondary if on the main sequence. For stars with no magnitudes in one filter, we assume the color difference to be zero to place them on the color-magnitude diagram.

FV CMa (HD 54309, HIP 34360, HR 2690, WDS J07074-2350) is a previously detected binary, with at least 8 epochs reported in the literature (see Tokovinin et al. 2021 for a summary). However, no orbital elements, or nature of the secondary are constrained in the literature. The currently available literature data are insufficient to compute reliable orbital periods. Adopting the same methods as previously, we constrain the secondary to a B8V spectral type assuming a coeval age to the primary (10 Myr).

QR Vul (HD192685, WDS J20153+2536, HIP 99824) is a previously known binary in Hartkopf et al. (2000). It also matches closely in separation with the observations using the PISCO (Pupil Interferometry Speckle COronagraph) speckle images (see summary in Scardia et al. 2006), who find the companion at multiple epochs (6 in total, when including this work). This companion has been known since 1879 and has ~ 30 observations noted in the WDS catalog.

Based on the available data and placing the objects on the CMD, the primary is $4.7 M_\odot$ star (spectral type of B3), with the secondary having a mass of $1.8 M_\odot$ (A3 type), assuming a coeval age of 100 Myr.

V2120 Cyg (HD 194883, HIP 100744) is a newly identified companion with no literature detections. The companion is located 75 au away, and appears to be on the main sequence as well. Assuming a coeval age, we sug-

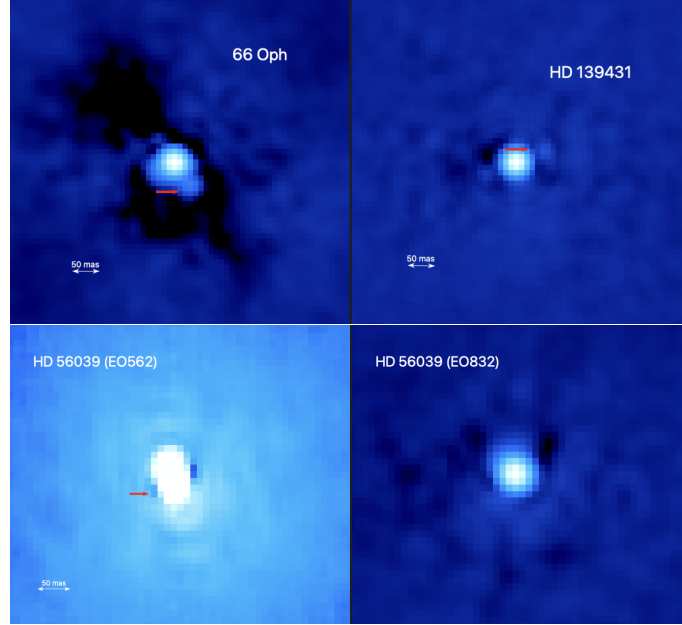


Figure 11. Zoomed-in reconstructed images for very close companions. The companion location is shown by the red arrow for 66 Oph (top left), HD 139431 (top right) in the EO832 filter, and in both EO 562 and EO 832 for HD 56039 in the bottom panel.

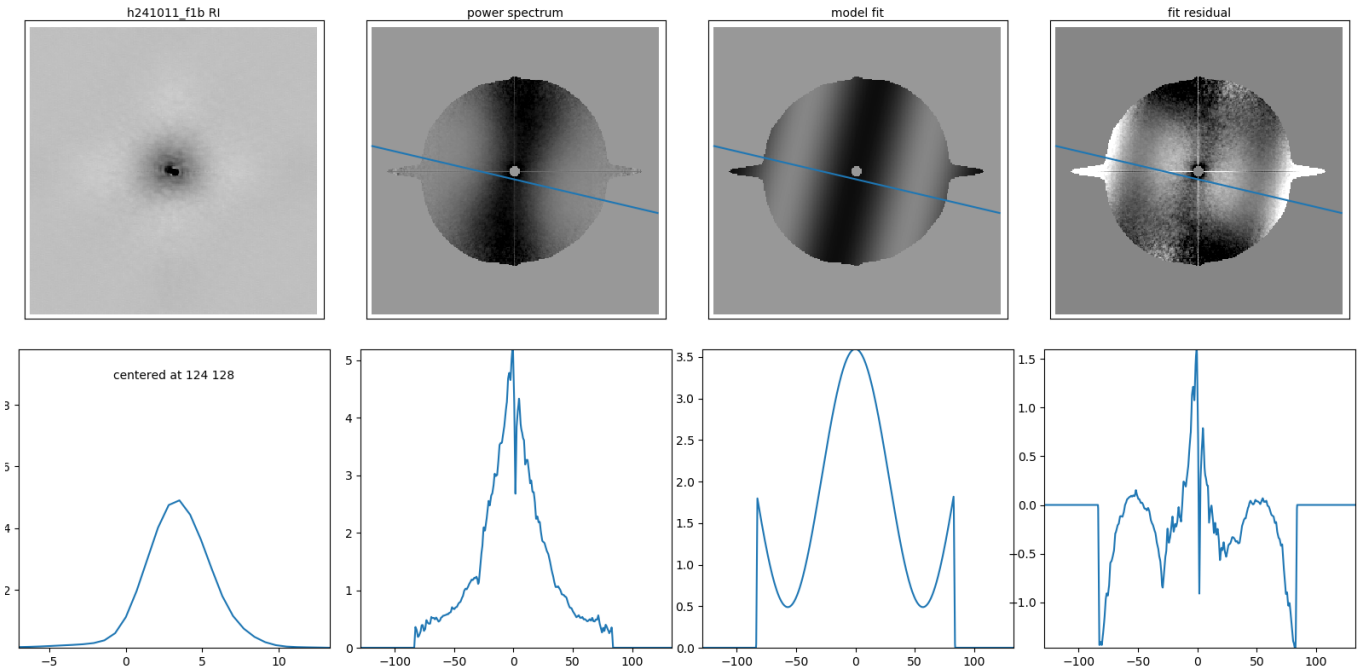


Figure 12. The image, power spectrum, model fit (accounting for the point source standard) and the residual are shown from the reduction steps for HD 56039 in the blue filter (top). The bottom panel shows the slice across the image (along the blue line in the top panel). The power spectrum fringe indicates the close-in companion.

gest a spectral type of B6V for the companion based on its mass.

CU Cir (HD 133495, HIP 74011) is newly identified companion, observed and detected only in the red camera. The companion is similar in mass (assuming coeval ages), given the small Δm of 0.68 mag, and in close orbit (86 au), but not interacting.

HD 59498 (HIP 36397) is newly identified companion detected in the EO 832 filter only, but observed with both cameras. The companion is faint, and must be at least mid-G given the Δm (estimated mass $\sim 0.8 M_{\odot}$).

OY Hya (HD 86612, HIP 48943, HR 3946) has been previously detected as a binary in the speckle observations of Tokovinin et al. (2021), with two epochs detected previously, including in Oudmaijer & Parr (2010). The companion was first resolved in Hipparcos data (1991.25). The companion is around 150 au away, and is very faint. It is not bluer than the primary, however is sufficiently blue that it is either likely a faint sdB star (unlikely given its distance to the primary), or a late type G-type ($\sim 1 M_{\odot}$) main-sequence companion.

CW Cir (HD 134958, HIP 74654) has a companion located 650 au away, observed and identified only in

EO 832. It is included in the catalog of Bodensteiner et al. (2020a) but they do not detect the binary given it's distance from the primary, and their focus on close spectroscopic companions. The companion is faint compared to the binary, but must be an early A spectral type based on the difference in magnitudes.

CK Cir (HD 128293, HIP 71668) is a newly identified companion found only in the red camera (observed only with). The companion is between late B-early A, and is located 700 au away.

QV Tel (HD 167128, HR 6819). Although not part of our final catalog of binaries, we observed QV Tel as part of our observations and detected no binarity in speckle imaging in only the EO 832 filter, agreeing with recent suggestion of a inner stripped star (Frost et al. 2022). We suggest that the detection in Klement et al. (2021a) could be of the reference star, HR 6622 which has a newly detected companion at similar separation and PA as reported for HR 6819, and is now a quadruple (prv. comm. A. Tokovinin) as indicated by a re-analysis of the existing multiple epoch data. Further deeper data of the primary in multiple filters can help ascertain this.

REFERENCES

- Abt, H. A. 2005, ApJ, 629, 507, doi: [10.1086/431207](https://doi.org/10.1086/431207)
- Abt, H. A., & Cardona, O. 1984, ApJ, 285, 190, doi: [10.1086/162490](https://doi.org/10.1086/162490)
- Abt, H. A., & Levy, S. G. 1978, ApJS, 36, 241, doi: [10.1086/190498](https://doi.org/10.1086/190498)
- Bailer-Jones, C. A. L., Rybizki, J., Fouesneau, M., Demleitner, M., & Andrae, R. 2021, AJ, 161, 147, doi: [10.3847/1538-3881/abd806](https://doi.org/10.3847/1538-3881/abd806)
- Belokurov, V., Penoyre, Z., Oh, S., et al. 2020, MNRAS, 496, 1922, doi: [10.1093/mnras/staa1522](https://doi.org/10.1093/mnras/staa1522)
- Berger, D. H., & Gies, D. R. 2001, ApJ, 555, 364, doi: [10.1086/321461](https://doi.org/10.1086/321461)
- Bjorkman, K. S., Miroshnichenko, A. S., McDavid, D., & Pogrosheva, T. M. 2002, ApJ, 573, 812, doi: [10.1086/340751](https://doi.org/10.1086/340751)
- Bodensteiner, J., Shenar, T., & Sana, H. 2020a, A&A, 641, A42, doi: [10.1051/0004-6361/202037640](https://doi.org/10.1051/0004-6361/202037640)
- Bodensteiner, J., Shenar, T., Mahy, L., et al. 2020b, A&A, 641, A43, doi: [10.1051/0004-6361/202038682](https://doi.org/10.1051/0004-6361/202038682)
- Boubert, D., & Evans, N. W. 2018, MNRAS, 477, 5261, doi: [10.1093/mnras/sty980](https://doi.org/10.1093/mnras/sty980)
- Chen, P. S., Liu, J. Y., & Shan, H. G. 2016, MNRAS, 463, 1162, doi: [10.1093/mnras/stw1757](https://doi.org/10.1093/mnras/stw1757)
- Cifuentes, C., Caballero, J. A., González-Payo, J., et al. 2025, A&A, 693, A228, doi: [10.1051/0004-6361/202452527](https://doi.org/10.1051/0004-6361/202452527)
- Correia, S., Zinnecker, H., Ratzka, T., & Sterzik, M. F. 2006, A&A, 459, 909, doi: [10.1051/0004-6361:20065545](https://doi.org/10.1051/0004-6361:20065545)
- Cruz-González, C., Recillas-Cruz, E., Costero, R., Peimbert, M., & Torres-Peimbert, S. 1974, RMxAA, 1, 211
- Dodd, J. M., Oudmaijer, R. D., Radley, I. C., Vioque, M., & Frost, A. J. 2024, MNRAS, 527, 3076, doi: [10.1093/mnras/stad3105](https://doi.org/10.1093/mnras/stad3105)
- Dotter, A. 2016, ApJS, 222, 8, doi: [10.3847/0067-0049/222/1/8](https://doi.org/10.3847/0067-0049/222/1/8)
- Evans, D. S., & Edwards, D. A. 1981, AJ, 86, 1277, doi: [10.1086/113008](https://doi.org/10.1086/113008)
- Fitton, S., Tofflemire, B. M., & Kraus, A. L. 2022, Research Notes of the American Astronomical Society, 6, 18, doi: [10.3847/2515-5172/ac4bb7](https://doi.org/10.3847/2515-5172/ac4bb7)
- Frost, A. J., Bodensteiner, J., Rivinius, T., et al. 2022, A&A, 659, L3, doi: [10.1051/0004-6361/202143004](https://doi.org/10.1051/0004-6361/202143004)

- Frost, A. J., Sana, H., Le Bouquin, J.-B., et al. 2025, arXiv e-prints, arXiv:2505.02300,
doi: [10.48550/arXiv.2505.02300](https://doi.org/10.48550/arXiv.2505.02300)
- Gaia Collaboration, Brown, A. G. A., Vallenari, A., et al. 2018, *A&A*, 616, A1, doi: [10.1051/0004-6361/201833051](https://doi.org/10.1051/0004-6361/201833051)
- Gaia Collaboration, Vallenari, A., Brown, A. G. A., et al. 2023, *A&A*, 674, A1, doi: [10.1051/0004-6361/202243940](https://doi.org/10.1051/0004-6361/202243940)
- Guerrero, C. A., Souza, T. B., Borges Fernandes, M., & Guajardo Jurado, A. D. 2025, *AJ*, 169, 251,
doi: [10.3847/1538-3881/adbf11](https://doi.org/10.3847/1538-3881/adbf11)
- Hartkopf, W. I., Tokovinin, A., & Mason, B. D. 2012, *AJ*, 143, 42, doi: [10.1088/0004-6256/143/2/42](https://doi.org/10.1088/0004-6256/143/2/42)
- Hartkopf, W. I., Mason, B. D., McAlister, H. A., et al. 2000, *AJ*, 119, 3084, doi: [10.1086/301402](https://doi.org/10.1086/301402)
- Horch, E., Ninkov, Z., & Franz, O. G. 2001, *AJ*, 121, 1583,
doi: [10.1086/319423](https://doi.org/10.1086/319423)
- Horch, E. P., Gomez, S. C., Sherry, W. H., et al. 2011, *AJ*, 141, 45, doi: [10.1088/0004-6256/141/2/45](https://doi.org/10.1088/0004-6256/141/2/45)
- Horch, E. P., van Belle, G. T., Davidson, Jr., J. W., et al. 2020, *AJ*, 159, 233, doi: [10.3847/1538-3881/ab87a6](https://doi.org/10.3847/1538-3881/ab87a6)
- Howell, S. B., Everett, M. E., Sherry, W., Horch, E., & Ciardi, D. R. 2011, *AJ*, 142, 19,
doi: [10.1088/0004-6256/142/1/19](https://doi.org/10.1088/0004-6256/142/1/19)
- Howell, S. B., Martínez-Vázquez, C. E., Furlan, E., et al. 2025, *Frontiers in Astronomy and Space Sciences*, 12, 1608411, doi: [10.3389/fspas.2025.1608411](https://doi.org/10.3389/fspas.2025.1608411)
- Hutter, D. J., Tycner, C., Zavala, R. T., et al. 2021, *ApJS*, 257, 69, doi: [10.3847/1538-4365/ac23cb](https://doi.org/10.3847/1538-4365/ac23cb)
- Kalari, V. M. 2019, *MNRAS*, 484, 5102,
doi: [10.1093/mnras/stz250](https://doi.org/10.1093/mnras/stz250)
- Kalari, V. M., Salinas, R., Zinnecker, H., et al. 2024, *ApJ*, 972, 3, doi: [10.3847/1538-4357/ad5bd9](https://doi.org/10.3847/1538-4357/ad5bd9)
- Kalari, V. M., Vink, J. S., de Wit, W. J., Bastian, N. J., & Méndez, R. A. 2019, *A&A*, 625, L2,
doi: [10.1051/0004-6361/201935107](https://doi.org/10.1051/0004-6361/201935107)
- Kervella, P., Arenou, F., & Thevenin, F. 2021, *VizieR Online Data Catalog: Stellar and substellar companions from Gaia EDR3* (Kervella+, 2022), *VizieR On-line Data Catalog: J/A+A/657/A7*. Originally published in: 2022A&A...657A...7K, doi: [10.26093/cds/vizier.36570007](https://doi.org/10.26093/cds/vizier.36570007)
- Klement, R., Scott, N., Rivinius, T., Baade, D., & Hadrava, P. 2021a, *The Astronomer's Telegram*, 14340, 1
- Klement, R., Hadrava, P., Rivinius, T., et al. 2021b, *ApJ*, 916, 24, doi: [10.3847/1538-4357/ac062c](https://doi.org/10.3847/1538-4357/ac062c)
- Klement, R., Schaefer, G. H., Gies, D. R., et al. 2022, *ApJ*, 926, 213, doi: [10.3847/1538-4357/ac4266](https://doi.org/10.3847/1538-4357/ac4266)
- Klement, R., Rivinius, T., Gies, D. R., et al. 2024, *ApJ*, 962, 70, doi: [10.3847/1538-4357/ad13ec](https://doi.org/10.3847/1538-4357/ad13ec)
- Koubský, P., Kotková, L., Votruba, V., Šlechta, M., & Dvořáková, Š. 2012, *A&A*, 545, A121,
doi: [10.1051/0004-6361/201219679](https://doi.org/10.1051/0004-6361/201219679)
- Koubský, P., Harmanec, P., Hubert, A. M., et al. 2000, *A&A*, 356, 913
- Lester, K. V., Matson, R. A., Howell, S. B., et al. 2021, *AJ*, 162, 75, doi: [10.3847/1538-3881/ac0d06](https://doi.org/10.3847/1538-3881/ac0d06)
- Lindgren, L., Hernández, J., Bombrun, A., et al. 2018, *A&A*, 616, A2, doi: [10.1051/0004-6361/201832727](https://doi.org/10.1051/0004-6361/201832727)
- Lindgren, L., Klioner, S. A., Hernández, J., et al. 2021, *A&A*, 649, A2, doi: [10.1051/0004-6361/202039709](https://doi.org/10.1051/0004-6361/202039709)
- Lindroos, K. P. 1986, *A&A*, 156, 223
- Martin, R. G., & Franchini, A. 2019, *MNRAS*, 489, 1797,
doi: [10.1093/mnras/stz2250](https://doi.org/10.1093/mnras/stz2250)
- Mason, B. D., ten Brummelaar, T., Gies, D. R., Hartkopf, W. I., & Thaller, M. L. 1997, *AJ*, 114, 2112,
doi: [10.1086/118630](https://doi.org/10.1086/118630)
- Mason, B. D., Wycoff, G. L., Hartkopf, W. I., Douglass, G. G., & Worley, C. E. 2022, *VizieR Online Data Catalog: The Washington Visual Double Star Catalog (Mason+ 2001-2020)*, *VizieR On-line Data Catalog: B/wds*. Originally published in: 2001AJ....122.3466M
- Moe, M., & Di Stefano, R. 2017, *ApJS*, 230, 15,
doi: [10.3847/1538-4365/aa6fb6](https://doi.org/10.3847/1538-4365/aa6fb6)
- Moffat, A. F. J., Marchenko, S. V., Seggewiss, W., et al. 1998, *A&A*, 331, 949
- Naoz, S. 2016, *ARA&A*, 54, 441,
doi: [10.1146/annurev-astro-081915-023315](https://doi.org/10.1146/annurev-astro-081915-023315)
- Offner, S. S. R., Moe, M., Kratter, K. M., et al. 2023, in *Astronomical Society of the Pacific Conference Series*, Vol. 534, *Protostars and Planets VII*, ed. S. Inutsuka, Y. Aikawa, T. Muto, K. Tomida, & M. Tamura, 275,
doi: [10.48550/arXiv.2203.10066](https://doi.org/10.48550/arXiv.2203.10066)
- Oudmaijer, R. D., & Parr, A. M. 2010, *MNRAS*, 405, 2439,
doi: [10.1111/j.1365-2966.2010.16609.x](https://doi.org/10.1111/j.1365-2966.2010.16609.x)
- Pecaut, M. J., & Mamajek, E. E. 2013, *ApJS*, 208, 9,
doi: [10.1088/0067-0049/208/1/9](https://doi.org/10.1088/0067-0049/208/1/9)
- Pomohaci, R., Oudmaijer, R. D., & Goodwin, S. P. 2019, *MNRAS*, 484, 226, doi: [10.1093/mnras/stz014](https://doi.org/10.1093/mnras/stz014)
- Pourbaix, D., Tokovinin, A. A., Batten, A. H., et al. 2004, *A&A*, 424, 727, doi: [10.1051/0004-6361:20041213](https://doi.org/10.1051/0004-6361:20041213)
- Radley, I. C., Oudmaijer, R. D., Vioque, M., & Dodd, J. M. 2025, *MNRAS*, 539, 1964, doi: [10.1093/mnras/staf618](https://doi.org/10.1093/mnras/staf618)
- Richards, M. T., Koubský, P., Šimon, V., et al. 2000, *ApJ*, 531, 1003, doi: [10.1086/308491](https://doi.org/10.1086/308491)
- Rivinius, T., Carciofi, A. C., & Martayan, C. 2013, *A&A Rv*, 21, 69, doi: [10.1007/s00159-013-0069-0](https://doi.org/10.1007/s00159-013-0069-0)
- Rivinius, T., & Klement, R. 2024, arXiv e-prints, arXiv:2411.06882, doi: [10.48550/arXiv.2411.06882](https://doi.org/10.48550/arXiv.2411.06882)

- Rivinius, T., Štefl, S., & Baade, D. 2006, A&A, 459, 137, doi: [10.1051/0004-6361:20053008](https://doi.org/10.1051/0004-6361:20053008)
- Rizzuto, A. C., Ireland, M. J., Robertson, J. G., et al. 2013, MNRAS, 436, 1694, doi: [10.1093/mnras/stt1690](https://doi.org/10.1093/mnras/stt1690)
- Ruban, E. V., Alekseeva, G. A., Arkharov, A. A., et al. 2006, Astronomy Letters, 32, 604, doi: [10.1134/S1063773706090052](https://doi.org/10.1134/S1063773706090052)
- Sana, H., Gosset, E., & Evans, C. J. 2009, MNRAS, 400, 1479, doi: [10.1111/j.1365-2966.2009.15545.x](https://doi.org/10.1111/j.1365-2966.2009.15545.x)
- Scardia, M., Prieur, J. L., Pansecchi, L., et al. 2006, MNRAS, 367, 1170, doi: [10.1111/j.1365-2966.2006.10035.x](https://doi.org/10.1111/j.1365-2966.2006.10035.x)
- Schmidt, M. 1968, ApJ, 151, 393, doi: [10.1086/149446](https://doi.org/10.1086/149446)
- Scott, N. J., Howell, S. B., Gnilka, C. L., et al. 2021, Frontiers in Astronomy and Space Sciences, 8, 138, doi: [10.3389/fspas.2021.716560](https://doi.org/10.3389/fspas.2021.716560)
- Skiff, B. A. 2010, VizieR Online Data Catalog: Catalogue of Stellar Spectral Classifications (Skiff, 2009-2012), VizieR On-line Data Catalog: B/mk. Originally published in: 2009yCat....1.2023S
- Souza, T. B., Guerrero, C. A., & Borges Fernandes, M. 2020, AJ, 159, 132, doi: [10.3847/1538-3881/ab6dcd](https://doi.org/10.3847/1538-3881/ab6dcd)
- Suffak, M. W., Jones, C. E., & Carciofi, A. C. 2025, MNRAS, 536, 2234, doi: [10.1093/mnras/stae2709](https://doi.org/10.1093/mnras/stae2709)
- Tokovinin, A. 2023, AJ, 165, 180, doi: [10.3847/1538-3881/acc464](https://doi.org/10.3847/1538-3881/acc464)
- Tokovinin, A., Mason, B. D., & Hartkopf, W. I. 2010, AJ, 139, 743, doi: [10.1088/0004-6256/139/2/743](https://doi.org/10.1088/0004-6256/139/2/743)
- Tokovinin, A., Mason, B. D., Mendez, R. A., et al. 2021, AJ, 162, 41, doi: [10.3847/1538-3881/ac00bd](https://doi.org/10.3847/1538-3881/ac00bd)
- Vioque, M., Oudmaijer, R. D., Schreiner, M., et al. 2020, A&A, 638, A21, doi: [10.1051/0004-6361/202037731](https://doi.org/10.1051/0004-6361/202037731)
- Wang, L., Gies, D. R., & Peters, G. J. 2017, ApJ, 843, 60, doi: [10.3847/1538-4357/aa740a](https://doi.org/10.3847/1538-4357/aa740a)
- . 2018, ApJ, 853, 156, doi: [10.3847/1538-4357/aaa4b8](https://doi.org/10.3847/1538-4357/aaa4b8)
- Wang, L., Gies, D. R., Peters, G. J., & Han, Z. 2023, AJ, 165, 203, doi: [10.3847/1538-3881/acc6ca](https://doi.org/10.3847/1538-3881/acc6ca)
- Wood, M. L., Mann, A. W., & Kraus, A. L. 2021, AJ, 162, 128, doi: [10.3847/1538-3881/ac0ae9](https://doi.org/10.3847/1538-3881/ac0ae9)
- Zheng, Z., Cao, Z., Deng, H., et al. 2023, ApJS, 266, 18, doi: [10.3847/1538-4365/acc94e](https://doi.org/10.3847/1538-4365/acc94e)